

# Ortho-Selective C–H Activation of Substituted Benzenes Effected by a Tungsten Alkylidene Complex without Substituent Coordination

Jenkins Y. K. Tsang, Miriam S. A. Buschhaus, Peter Legzdins,\* and Brian O. Patrick

Department of Chemistry, The University of British Columbia, Vancouver,  
British Columbia, Canada V6T 1Z1

Received May 8, 2006

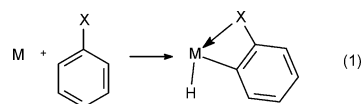
Gentle thermolysis of the bis(neopentyl) complex  $\text{Cp}^*\text{W}(\text{NO})(\text{CH}_2\text{CMe}_3)_2$  (**1**) at 70 °C in various substituted benzenes results in the loss of neopentane and the generation of the transient alkylidene complex  $\text{Cp}^*\text{W}(\text{NO})(=\text{CHCMe}_3)$  (**A**), which subsequently effects single C–H bond activations of the benzenes. These activations exhibit a pronounced selectivity for the C–H linkages ortho to the benzene substituents. Thus, thermal reactions of **1** with  $\text{C}_6\text{H}_5\text{X}$  lead to the preferential formation of the corresponding  $\text{Cp}^*\text{W}(\text{NO})(\text{CH}_2\text{CMe}_3)(o\text{-C}_6\text{H}_4\text{X})$  complexes, the ortho-selectivity, i.e.,  $\text{X} = \text{F} > \text{OMe} > \text{Cl} > \text{Br} > \text{C}\equiv\text{CPh}$ , diminishing as the steric demands of the substituents increase. Consistently, thermolyses of **1** in  $o\text{-C}_6\text{H}_4\text{X}_2$  afford  $\text{Cp}^*\text{W}(\text{NO})(\text{CH}_2\text{CMe}_3)(2,3\text{-C}_6\text{H}_3\text{X}_2)$  complexes with 98% selectivity when  $\text{X} = \text{F}$  and 82% selectivity when  $\text{X} = \text{Cl}$ . Similarly, the principal organometallic products resulting from the thermolyses of **1** in  $m\text{-C}_6\text{H}_4\text{X}_2$  are the ortho-para-activated isomers  $\text{Cp}^*\text{W}(\text{NO})(\text{CH}_2\text{CMe}_3)(2,4\text{-C}_6\text{H}_3\text{X}_2)$  with 84% selectivity when  $\text{X} = \text{F}$  and 89% selectivity when  $\text{X} = \text{Cl}$ . Finally, thermolyses of **1** in para-disubstituted benzenes  $p\text{-C}_6\text{H}_4\text{XY}$  ( $\text{X} = \text{F}$  or  $\text{OMe}$ ,  $\text{Y} = \text{Cl}$  or  $\text{OMe}$ ) again reveal that the ortho-directing abilities of the substituents diminish in the order  $\text{F} > \text{OMe} > \text{Cl}$ . Some mechanistic insights into these activation processes have been obtained by monitoring of the early stages of the thermolysis of **1** in chlorobenzene by  $^1\text{H}$  NMR spectroscopy. This monitoring reveals that the selectivity of the alkylidene intermediate **A** for forming the ortho-activated isomer is thermodynamic rather than kinetic in nature. Thus, the meta- and para-activated isomers are formed initially, but then convert to the ortho-activated product. The principal organometallic complexes resulting from ortho-C–H activations are formally 16-electron species in which there are no interactions between the tungsten centers and the Lewis-basic benzene substituents. Instead, the Lewis-acidic tungsten centers engage in intramolecular agostic interactions with the methylene C–H bonds of their neopentyl ligands to acquire some additional electron density. Being coordinatively and electronically unsaturated, these tungsten complexes react readily with added Lewis bases. Thus, treatment of  $\text{Cp}^*\text{W}(\text{NO})(\text{CH}_2\text{CMe}_3)(o\text{-C}_6\text{H}_4\text{F})$  with  $\text{Et}_4\text{NCN}$  and  $\text{CO}$  produces  $[\text{Et}_4\text{N}]^+[\text{Cp}^*\text{W}(\text{NO})(\text{CH}_2\text{CMe}_3)(\text{CN})(o\text{-C}_6\text{H}_4\text{F})]^-$  and  $\text{Cp}^*\text{W}(\text{NO})(\eta^2\text{-C}(=\text{O})\text{CH}_2\text{CMe}_3)(o\text{-C}_6\text{H}_4\text{F})$ , respectively, and the solid-state molecular structure of the latter complex has also been established by a single-crystal X-ray crystallographic analysis.

## Introduction

The activation and functionalization of C–H bonds at transition-metal centers continue to attract the attention of researchers worldwide since these processes hold the promise of leading to efficient and catalytic methods for the selective conversion of hydrocarbon feedstocks into functionalized organic compounds. Considerable progress in this regard has been made in the past 25 years, and numerous metal-containing complexes have been discovered to effect intermolecular C–H bond activations, often selectively and under relatively mild conditions.<sup>1</sup> Notable examples include late transition-metal complexes that oxidatively add C–H linkages to the metal center, transition-metal, lanthanide, and actinide complexes that facilitate C–H activation via M–C  $\sigma$ -bond metathesis, and

early- to mid-transition-metal complexes that add C–H bonds across M=N and M=C linkages. A fundamental understanding of these discrete C–H activation processes has been acquired for many of these complexes, and the chemistry of some systems has been significantly advanced toward efficient, catalytic functionalizations.<sup>1</sup>

Particularly important from a synthetic point of view is the regioselective activation of strong C–H bonds in the presence of potentially reactive substituents. One of the notable successes in this area has been the activation of aryl C–H bonds ortho to a substituent that is capable of acting as a Lewis base (eq 1).<sup>2,3</sup>

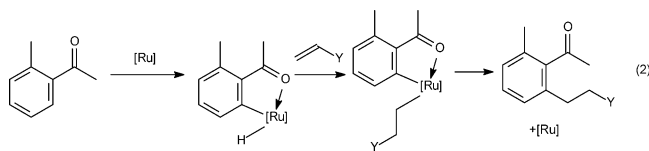


The substituent (X) can play one of two roles in these processes. It may first coordinate to the metal center and thereby direct and facilitate the activation to the ortho C–H linkage. Such is the case during the activation of some haloarenes<sup>2a,3b</sup> as well as the Ru(0)-catalyzed “site-directed” addition of the

\* To whom correspondence should be addressed. E-mail: legzdins@chem.ubc.ca.

(1) For recent books and reviews on the topic of C–H activation, see: (a) *Activation and Functionalization of C–H Bonds*; Goldberg, K. I., Goldman, A. S., Eds.; ACS Symposium Series 885; American Chemical Society: Washington, DC, 2004. (b) Arndtsen, B. A.; Bergman, R. G.; Mobley, T. A.; Peterson, T. H. *Acc. Chem. Res.* **1995**, *28*, 154. (c) Shilov, A. E.; Shul'pin, G. B. *Chem. Rev.* **1997**, *97*, 2879. (d) Labinger, J. A.; Bercaw, J. E. *Nature* **2002**, *417*, 507.

ortho C–H bonds of aromatic ketones to olefins developed by Murai and co-workers, a particular example of which is shown in eq 2.<sup>4</sup>



Alternatively, the substituent X in eq 1 may simply stabilize the product complex by coordination to the metal center after the C–H activation process has been effected. Such is the case during the selective addition of the ortho C–H bonds of nitrobenzene and acetophenone to a (PCP)Ir center recently reported by Goldman and co-workers.<sup>2b</sup> In either case, the end result of the transformations summarized in eq 1 is that X occupies a position in the metal's coordination sphere that may well be needed for subsequent derivatization of the activated arene.

Our contributions to this area of chemistry began with our discovery that Cp\**M*(NO)(hydrocarbyl)<sub>2</sub> complexes (Cp\* = η<sup>5</sup>-C<sub>5</sub>Me<sub>5</sub>) of molybdenum and tungsten exhibit hydrocarbyl-dependent thermal chemistry.<sup>5</sup> Thus, gentle thermolysis of appropriate Cp\**M*(NO)(hydrocarbyl)<sub>2</sub> precursors (M = Mo, W) results in loss of hydrocarbon and the transient formation of 16-electron organometallic complexes such as Cp\**M*(NO)-(alkylidene), Cp\**M*(NO)(η<sup>2</sup>-allene), and Cp\**M*(NO)(η<sup>2</sup>-benzynes). These intermediates first effect the single activation of hydrocarbon C–H bonds intermolecularly via the reverse of the transformations by which they were generated. Some of the new product complexes formed in this manner are stable and may be isolated. Others are thermally unstable under the experimental conditions employed and react further to effect double or triple C–H bond activations of the hydrocarbon substrates. In this report we present the results of our investigations of the thermal chemistry of Cp\**W*(NO)(=CHCMe<sub>3</sub>) (**A**) (generated by gentle thermolysis of Cp\**W*(NO)(CH<sub>2</sub>CMe<sub>3</sub>)<sub>2</sub> (**1**))<sup>6</sup> with a series of mono- and disubstituted benzenes, and we compare these results with related studies conducted previously by us and others. We have established that **A** exhibits good selectivity for C–H activation of the substrates at the ortho position and that functional groups as weakly basic as a C≡C bond or a fluorine atom can serve as the ortho-directing group. Most interestingly, this selectivity is thermodynamic in nature and does not involve coordination of the ortho-directing substituent to the tungsten center.

(2) Selected recent examples of ortho-C–H activation: (a) Ben-Ari, E.; Cohen, R.; Gandelman, M.; Shimon, L. J. W.; Martin, J. M. L.; Milstein, D. *Organometallics* **2006**, *25*, 3190, and references therein. (b) Zhang, X.; Kanzelberger, M.; Emge, T. J.; Goldman, A. S. *J. Am. Chem. Soc.* **2004**, *126*, 13192–13193. (c) Zhang, F.; Kirby, C. W.; Hairshine, D. W.; Jennings, M. C.; Puddephatt, R. J. *J. Am. Chem. Soc.* **2005**, *127*, 14196. (d) Renkema, K. B.; Bosque, R.; Streib, W. E.; Maseras, F.; Eisenstein, O.; Caulton, K. G. *J. Am. Chem. Soc.* **1999**, *121*, 10895. (e) Hill, A. F.; Schultz, M.; Willis, A. C. *Organometallics* **2004**, *23*, 5729, and references therein. (f) Eguillor, B.; Esteruelas, M. A.; Oliván, M.; Onate, E. *Organometallics* **2004**, *23*, 6015.

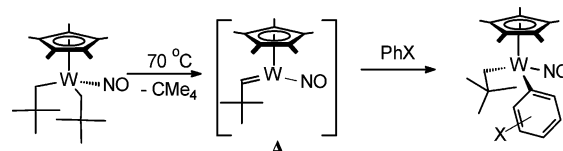
(3) For recent examples of a metal complex capable of both C–H and C–X (X = halogen) activation, see: (a) Fan, L.; Parkin, S.; Ozerov, O. V. *J. Am. Chem. Soc.* **2005**, *127*, 16772. (b) We, F.; Dash, A. K.; Jordan, R. F. *J. Am. Chem. Soc.* **2004**, *126*, 15360.

(4) Kakiuchi, F.; Murai, S. *Acc. Chem. Res.* **2002**, *35*, 826.

(5) Pamplin, C. B.; Legzdins, P. *Acc. Chem. Res.* **2003**, *36*, 223, and references therein.

(6) Adams, C. S.; Legzdins, P.; Tran, E. *J. Am. Chem. Soc.* **2001**, *123*, 612.

Scheme 1



Compound	X	ortho : meta : para
<b>2a-c</b>	F	97 : 2 : 1
<b>3a-c</b>	Cl	75 : 18 : 7
<b>4a-c</b>	Br	63 : 25 : 12
<b>5a-c</b>	OMe	87 : 7 : 6
<b>6a-c</b>	C=CPh	51 : 33 : 16

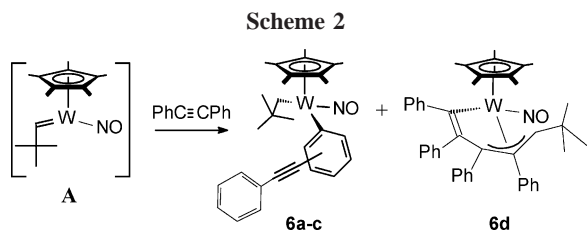
## Results and Discussion

**C–H Activation of Monosubstituted Benzenes.** Scheme 1 summarizes the C–H bond activations that occur when Cp\**W*(NO)(CH<sub>2</sub>CMe<sub>3</sub>)<sub>2</sub> (**1**) is thermolyzed in various monosubstituted benzenes. Thus, thermolysis of **1** in a monohalobenzene C<sub>6</sub>H<sub>5</sub>X (X = F, Cl, or Br) at 70 °C for 40 h results in the formation of the ortho-, meta-, and para-activated isomers Cp\**W*(NO)(CH<sub>2</sub>CMe<sub>3</sub>)(C<sub>6</sub>H<sub>4</sub>X) (X = F, **2a-c**; X = Cl, **3a-c**; X = Br, **4a-c**), with the ortho-activated isomer being formed in the greatest amount in all cases. There is no evidence for the occurrence of concomitant C–X activations during these transformations.<sup>3</sup> We have previously shown that steric factors play a significant role in determining the regioselectivities of C–H activation of alkylated arenes effected by **A**.<sup>7</sup> For example, thermolysis of **1** in toluene (PhCH<sub>3</sub>) results in the formation of the ortho-, meta-, and para-activated isomers in an *o*:*m*:*p* ratio of 1:59:40, in addition to organometallic products (~19%) resulting from the benzylic C–H activation of toluene. Similarly, thermolysis of **1** in α,α,α-trifluorotoluene (PhCF<sub>3</sub>) affords an *o*:*m*:*p* ratio of 0:65:35. These results demonstrate that a bulky group effectively discourages ortho C–H activation. In the case of the haloarenes, however, **A** exhibits a preference for ortho C–H activation despite the steric hindrance imposed by the halogen substituent. Hence, there must be an electronic factor operative as well during these activations (*vide infra*).

During these activations by the tungsten complex, fluorobenzene gives excellent regioselectivity (97% ortho), whereas chlorobenzene (75% ortho) and bromobenzene (63% ortho) are less selective in this regard. This trend of F > Cl > Br contrasts with the selectivity exhibited by [(PNP)Ir(cyclooctene)]<sup>+</sup>BF<sub>4</sub><sup>−</sup> (PNP = 2,6-bis(*di-tert*-butylphosphinomethyl)pyridine).<sup>2a</sup> The cationic iridium complex displays a pronounced preference for the ortho C–H bonds of bromobenzene, the *o*:*m*:*p* ratio being 70:20:10 when the iridium reactant has been completely consumed; prolonged heating of the final reaction mixture at 60 °C results in the quantitative formation of the ortho-activated complex as the only product. On the other hand, the iridium complex shows no regioselectivity toward the C–H bonds of fluorobenzene and forms a statistical mixture of the ortho-, meta-, and para-activated isomers.<sup>2a</sup>

Thermolysis of **1** in anisole also results in the formation of the ortho-, meta-, and para-activated isomers Cp\**W*(NO)(CH<sub>2</sub>CMe<sub>3</sub>)(C<sub>6</sub>H<sub>4</sub>OMe) (**5a-c**) with excellent selectivity for the ortho-activated isomer **5a** (87%). It is noteworthy that no organometallic product resulting from C–H activation of the methoxy group is evident in the final reaction mixture. Similar thermolysis of **1** in molten diphenylacetylene results in a slightly more complex mixture, as four organometallic complexes are formed in different amounts (Scheme 2). The principal product is the ortho-activated isomer Cp\**W*(NO)(CH<sub>2</sub>CMe<sub>3</sub>)(2-C<sub>6</sub>H<sub>4</sub>C≡

(7) Adams, C. S.; Legzdins, P.; Tran, E. *Organometallics* **2002**, *21*, 1474.



CPh) (**6a**, 51%). Two of the other complexes are believed to be the meta- and para-activated isomers on the basis of the chemical shifts and multiplicities of agostic and nonagostic neopentyl methylene proton signals evident in the  $^1\text{H}$  NMR spectrum of the crude product mixture (vide infra). However, significant overlapping of characteristic signals in the aryl region prevents definitive structural elucidation of these two complexes by  $^1\text{H}$  NMR spectroscopy. These two compounds, as well as complexes **2b,c**, **3b,c**, **4b,c**, and **5b,c**, also decompose on various chromatographic columns. Interestingly, a minor fourth complex can be successfully isolated in 5% yield from the product mixture by chromatography since it elutes in a narrow orange band ahead of all the other complexes. Crystallization from pentane yields plates, and a preliminary X-ray crystallographic analysis has revealed the identity of this fourth complex to be  $\text{Cp}^*\text{W}(\text{NO})(\eta^3, \eta^1\text{-}(\text{Me}_3\text{C})\text{HC-CPh}=\text{CPh}=\text{CPh}=\text{CPh})$  (**6d**). Unfortunately, the quality of the X-ray diffraction data is such that a meaningful discussion of the intramolecular metrical parameters of **6d** is not possible. Nevertheless, the atom connectivity in this compound has been unambiguously established, and it reveals that two diphenylacetylene molecules have been coupled within the coordination sphere of the tungsten center as shown in Scheme 2. Complex **6d** probably results from the [2+2] cycloaddition of one diphenylacetylene molecule to the  $\text{W}=\text{C}$  alkylidene linkage in transient intermediate **A** followed by a ring-expansion reaction involving the addition of a second diphenylacetylene molecule, before isomerization to the final allyl-vinyl complex. In any event, the formation of **6d** establishes that acetylenic  $\text{C}=\text{C}$  bonds are not totally immune from reacting with the  $\text{W}=\text{C}$  alkylidene linkage in **A**.<sup>8</sup>

In comparison, thermolysis of **1** in 3-hexyne affords only the coupled product analogous to **6d**, namely,  $\text{Cp}^*\text{W}(\text{NO})(\eta^3, \eta^1\text{-}(\text{Me}_3\text{C})\text{HC-CEt}=\text{CEt}=\text{CEt}=\text{CEt})$  (**7**), while compounds resulting from C–H activations of 3-hexyne are apparently not formed. Complex **7** has been subjected to a single-crystal, X-ray crystallographic analysis, and its solid-state molecular structure is shown in Figure 1.

**C–H Activation of Disubstituted Benzenes.** Thermolyses of **1** in *o*-difluorobenzene and *o*-dichlorobenzene both lead to ortho-selective C–H activation, the principal products being  $\text{Cp}^*\text{W}(\text{NO})(\text{CH}_2\text{CMe}_3)(2,3\text{-C}_6\text{H}_3\text{F}_2)$  (**8a**) and  $\text{Cp}^*\text{W}(\text{NO})(\text{CH}_2\text{CMe}_3)(2,3\text{-C}_6\text{H}_3\text{Cl}_2)$  (**9a**), respectively (Scheme 3). The product ratios of 98:2 and 82:18 for **8a:8b** and **9a:9b**, respectively, are consistent with the regioselectivities observed during the C–H activation of the respective monohalobenzenes (vide supra).

Not surprisingly, thermolyses of **1** in *m*-difluorobenzene and *m*-dichlorobenzene lead to different product ratios (Scheme 4). In the case of *m*-difluorobenzene, the major organometallic product is the ortho-para-activated isomer  $\text{Cp}^*\text{W}(\text{NO})(\text{CH}_2\text{CMe}_3)(2,4\text{-C}_6\text{H}_3\text{F}_2)$  (**10a**, 84%). The steric hindrance afforded by the second fluorine atom accounts for the relatively low yield of the ortho-ortho-activated isomer,  $\text{Cp}^*\text{W}(\text{NO})(\text{CH}_2\text{CMe}_3)(2,6\text{-}$

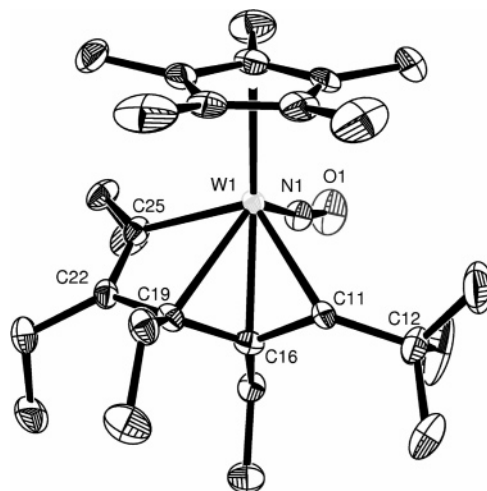
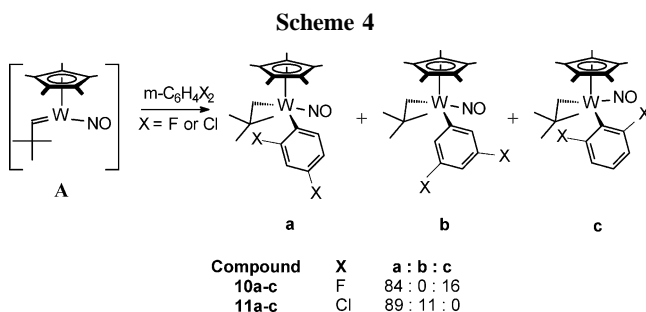
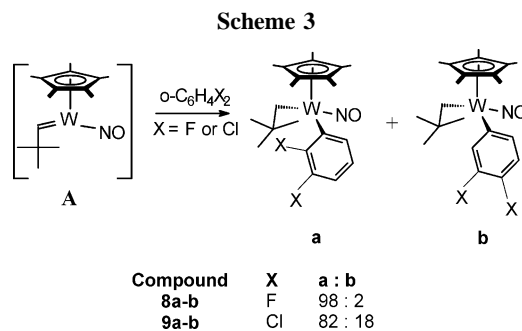
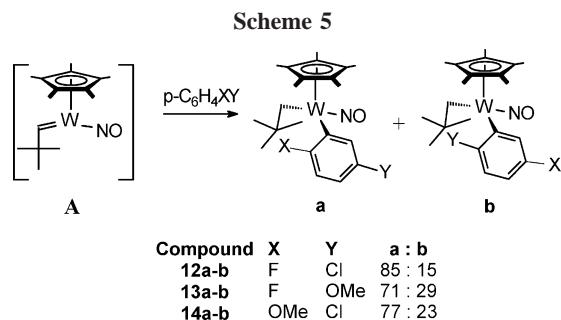


**Figure 1.** Solid-state molecular structure of  $\text{Cp}^*\text{W}(\text{NO})(\eta^3, \eta^1\text{-}(\text{Me}_3\text{C})\text{HC-CEt}=\text{CEt}=\text{CEt}=\text{CEt})$  (**7**) with 50% probability thermal ellipsoids shown. Selected interatomic distances (Å) and angles (deg):  $\text{W1-N1} = 1.785(4)$ ,  $\text{N1-O1} = 1.216(5)$ ,  $\text{W1-C11} = 2.328(4)$ ,  $\text{W1-C16} = 2.294(4)$ ,  $\text{W1-C19} = 2.396(4)$ ,  $\text{W1-C25} = 2.192(4)$ ,  $\text{C11-C16} = 1.456(6)$ ,  $\text{C16-C19} = 1.408(6)$ ,  $\text{C19-C22} = 1.498(6)$ ,  $\text{C22-C25} = 1.336(6)$ ,  $\text{W1-N1-O1} = 170.2(4)$ ,  $\text{C16-C19-C22} = 119.2(3)$ .



$\text{C}_6\text{H}_3\text{F}_2$ ) (**10c**, 16%), which can be separated from the major product by careful column chromatography on alumina. The meta-meta-activated isomer **10b** is not formed in any detectable amount. The distribution of products from this reaction suggests that the well-known acidity of the ortho protons in fluoroarenes does not play a significant role during these transformations, because if it did, then isomer **10c** would have been expected to be the major organometallic product.<sup>2d</sup> Thermolysis of **1** in *m*-dichlorobenzene, on the other hand, also affords the ortho-para-activated isomer,  $\text{Cp}^*\text{W}(\text{NO})(\text{CH}_2\text{CMe}_3)(2,4\text{-C}_6\text{H}_3\text{Cl}_2)$  (**11a**), as the major product (89%). The other product is the meta-meta-activated isomer,  $\text{Cp}^*\text{W}(\text{NO})(\text{CH}_2\text{CMe}_3)(3,5\text{-C}_6\text{H}_3\text{Cl}_2)$  (**11b**, 11%), while the very hindered ortho-ortho-position of *m*-dichlorobenzene is not activated at all. For comparison, it may be noted that we have previously shown that the thermolysis of **1** in mesitylene results exclusively in benzylic C–H activation products and no aryl C–H activation products.<sup>7</sup>

(8) To the best of our knowledge, coupling between two alkyne molecules and a metal–alkylidene linkage has not been reported previously, although the closely related  $\text{W}=\text{N}$  and  $\text{Mo}=\text{N}$  linkages have been shown to be able to react with a ring-strained alkyne such as cyclooctyne in a similar manner.<sup>9</sup>



Thermolyses of **1** in *p*-disubstituted benzenes have been conducted to determine how the functional groups compare with each other as the ortho-directing group for C–H activations, and they have established that the ortho-directing abilities of the substituents diminish in the order F > OMe > Cl, just as for the monosubstituted benzenes (vide supra). Thus, as shown in Scheme 5, thermolysis of **1** in *p*-chlorofluorobenzene produces Cp\*W(NO)(CH<sub>2</sub>CMe<sub>3</sub>)(C<sub>6</sub>H<sub>3</sub>-2-F-5-Cl) (**12a**) and Cp\*W(NO)(CH<sub>2</sub>CMe<sub>3</sub>)(C<sub>6</sub>H<sub>3</sub>-2-Cl-5-F) (**12b**) in an 85:15 ratio. Similarly, thermolysis of **1** in *p*-fluoroanisole affords Cp\*W(NO)(CH<sub>2</sub>CMe<sub>3</sub>)(C<sub>6</sub>H<sub>3</sub>-2-F-5-OMe) (**13a**) and Cp\*W(NO)(CH<sub>2</sub>CMe<sub>3</sub>)(C<sub>6</sub>H<sub>3</sub>-2-OMe-5-F) (**13b**) in a 71:29 ratio, while thermolysis of **1** in *p*-chloroanisole results in a 77:23 product ratio of the two isomers Cp\*W(NO)(CH<sub>2</sub>CMe<sub>3</sub>)(C<sub>6</sub>H<sub>3</sub>-2-OMe-5-Cl) (**14a**) and Cp\*W(NO)(CH<sub>2</sub>CMe<sub>3</sub>)(C<sub>6</sub>H<sub>3</sub>-2-Cl-5-OMe) (**14b**), respectively. Complete separation of the two isomers in each of the two latter reactions (i.e., **13a** and **13b**, and **14a** and **14b**) can be achieved by careful chromatography on activated alumina. Complexes **13a** and **13b** can be identified by their <sup>19</sup>F NMR spectra; however, no convenient spectroscopic method (e.g., a 1D selective NOE experiment) has yet been found that differentiates between **14a** and **14b**. The identities of the two isomers have thus been inferred from the observed product ratios, as well as from the colors and the solubility properties of the two complexes. All other complexes bearing an *o*-methoxyphenyl ligand in this study are magenta-purple and are only slightly soluble in *n*-pentane, while all complexes bearing an *o*-chlorophenyl ligand are red and much more soluble in the same solvent.

**Spectroscopic Properties of the C–H Activated Complexes.** The <sup>1</sup>H NMR spectra of all the nitrosyl complexes resulting from aryl C–H activation feature two diastereotopic methylene proton signals, with one signal appearing below δ = 0 ppm and the other appearing between δ = 4 and 6 ppm. These signals are much more upfield and downfield, respectively, than where methylene proton signals usually appear. The chemical shifts of these signals and their <sup>1</sup>J<sub>HC</sub> coupling constants (vide infra) suggest that there are agostic interactions between the tungsten centers and one of the methylene C–H bonds in these compounds.<sup>10</sup> This is a remarkable and unexpected feature of the ortho-activated complexes. It is not unreasonable to expect that the ortho halogen atoms in complexes **2a**, **3a**, or **4a**, the methoxy oxygen atom in **5a**, or the carbon–carbon triple bond in **6a** would be coordinated to the formally 16-electron metal center in the final products. However, the <sup>1</sup>H NMR data indicate that these Lewis-basic groups are not coordinated to tungsten in their respective complexes; otherwise the metal centers would have no need to engage in agostic interactions with methylene C–H bonds to acquire additional electron density.

For each of the complexes containing an *o*-fluorophenyl ligand, the agostic methylene proton signal appears as a doublet of doublets, the coupling constants being in the range of 11 and 6 Hz, respectively. The larger coupling is due to <sup>2</sup>J<sub>HH</sub>, but the smaller coupling can only be attributed to long-range interaction between this proton and the ortho fluorine atom. Such long-range coupling between an aryl ortho-fluoro group and an alkyl proton is rare, but not unprecedented.<sup>11–13</sup> Interestingly, the nonagostic methylene proton does not couple to the fluorine atom at all. Hence, the long-range coupling observed during this study may actually be occurring through space.<sup>13</sup> For comparison, the <sup>1</sup>H NMR spectrum of [Et<sub>4</sub>N]<sup>+</sup>[Cp\*W(NO)(CH<sub>2</sub>CMe<sub>3</sub>)(CN)(*o*-C<sub>6</sub>H<sub>4</sub>F)]<sup>−</sup> ([Et<sub>4</sub>N]<sup>+</sup> [**15**]<sup>−</sup>, vide infra), in which the *o*-fluorophenyl group and the neopentyl group are trans to each other in the tungsten's coordination sphere, does not exhibit such H–F coupling. Long-range H–F coupling has been found to be regioselective in certain cases, particularly when the *o*-fluorophenyl group is not freely rotating.<sup>12</sup>

The presence of long-range H–F coupling has been very useful for structure elucidation in a few cases. For example, complex **10c** can be unambiguously identified by the appearance of its agostic methylene proton signal in its <sup>1</sup>H NMR spectrum, namely, a doublet of triplets reflecting coupling of the agostic proton to the other methylene proton as well as to two apparently equivalent ortho fluorine atoms. In a similar manner complexes **12a** and **13a** can be readily differentiated from their isomers by the appearance of the agostic methylene proton signals, namely, doublets of doublets for **12a** and **13a** versus doublets for **12b** and **13b**.

Gated-<sup>13</sup>C NMR spectra have been recorded for several of the compounds, and they display features that are consistent with their <sup>1</sup>H NMR data and their proposed molecular structures. Specifically, the methylene carbon signals in the proton-coupled spectra appear as doublets of doublets, with the magnitude of the two <sup>1</sup>J<sub>CH</sub> coupling constants being in the range of 120 and 90 Hz, respectively. We have previously established that such coupling constants are diagnostic of agostic C–H interactions with the metal centers in complexes of this type.<sup>10</sup> Furthermore, the products obtained from the thermolysis of **1** in fluorinated arenes have also been characterized by <sup>19</sup>F NMR spectroscopy. Typically the signals due to the fluorine atoms that are ortho to W appear between 0 and −20 ppm (with reference to CF<sub>3</sub>COOH), while the signals due to the fluorine atoms that are meta or para to W occur between −40 and −50 ppm. The only exception to this generalization is the <sup>19</sup>F NMR spectrum of compound **8a**, which exhibits signals attributable to the ortho and meta fluorine atoms at −31.6 and −62.8 ppm, respectively. Such an upfield shift is commonly observed for compounds containing mutually ortho fluoro groups, as in the parent *o*-difluorobenzene and other *o*-difluorosubstituted arenes. Overall, the <sup>19</sup>F NMR data for the new complexes synthesized during the current investigation are consistent with their structural assignments.

**X-ray Crystallographic Analyses of the C–H Activated Complexes.** To establish the metrical parameters of the solid-state molecular structures of these types of alkyl aryl complexes, we have effected single-crystal X-ray crystallographic analyses on several representative compounds prepared during this study.

The solid-state molecular structures of piano-stool complexes **2a** and **5a** are very similar, and they are shown in Figures 2

(9) Lokare, K. S.; Ciszewski, J. T.; and Odom, A. L. *Organometallics* **2005**, *23*, 5386.

(10) Bau, R.; Mason, S. A.; Patrick, B. O.; Adams, C. S.; Sharp, W. B.; Legzdins, P. *Organometallics* **2001**, *20*, 4492.

(11) Kraft, B. M.; Lachicotte, R. J.; Jones, W. D. *Organometallics* **2002**, *21*, 727.

(12) Hughes, R. P.; Laritchev, R. B.; Williamson, A.; Incarvito, C. D.; Zakharov, L. N.; Rheingold, A. L. *Organometallics* **2003**, *22*, 2134.

(13) Crespo, M.; Font-Bardía, M.; Solans, X. *Polyhedron* **2002**, *21*, 105.

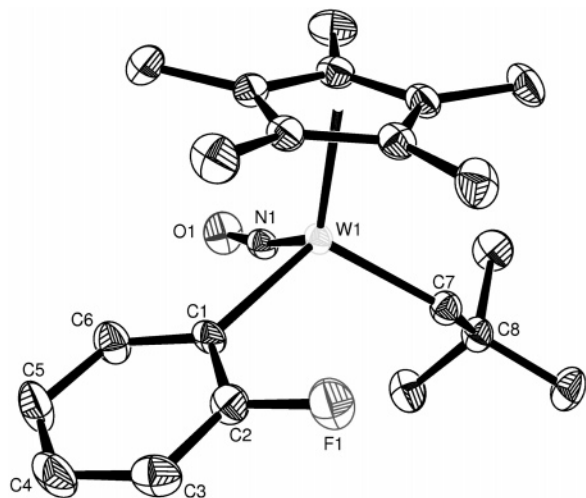


**Figure 2.** Solid-state molecular structure of  $\text{Cp}^*\text{W}(\text{NO})(\text{CH}_2\text{-CMe}_3)(o\text{-C}_6\text{H}_4\text{F})$  (**2a**) with 50% probability thermal ellipsoids shown. Selected interatomic distances (Å) and angles (deg):  $\text{W1-N1} = 1.775(2)$ ,  $\text{W1-C7} = 2.101(3)$ ,  $\text{W1-C1} = 2.162(3)$ ,  $\text{W1-F1} = 3.222$ ,  $\text{N1-O1} = 1.228(3)$ ,  $\text{W1-N1-O1} = 169.4(2)$ ,  $\text{W1-C7-C8} = 130.9(2)$ ,  $\text{W1-C1-C2} = 121.5(2)$ .

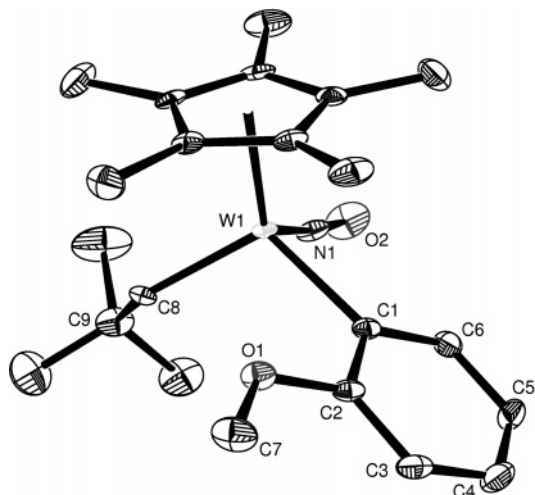


**Figure 3.** Solid-state molecular structure of  $\text{Cp}^*\text{W}(\text{NO})(\text{CH}_2\text{-CMe}_3)(o\text{-C}_6\text{H}_4\text{OMe})$  (**5a**) with 50% probability thermal ellipsoids shown. Selected interatomic distances (Å) and angles (deg):  $\text{W1-N1} = 1.765(3)$ ,  $\text{W1-C8} = 2.122(4)$ ,  $\text{W1-C1} = 2.149(3)$ ,  $\text{W1-O1} = 3.110$ ,  $\text{N1-O2} = 1.223(4)$ ,  $\text{W1-N1-O2} = 171.6(3)$ ,  $\text{W1-C8-C9} = 129.7(2)$ ,  $\text{W1-C1-C2} = 119.7(2)$ ,  $\text{C2-O1-C7} = 117.6(3)$ .

and 3, respectively. Both the fluoro and methoxy groups are located trans to the nitrosyl ligand (as opposed to the neopentyl ligand) in an orientation that brings these groups into the vicinity of the low-energy vacant orbital that is situated between the W-alkyl and W-aryl linkages in such 16-electron  $\text{Cp}^*\text{W}(\text{NO})$ -(alkyl)(aryl) compounds.<sup>14</sup> However, the W–F and W–O distances in the two complexes are 3.222 and 3.110 Å, respectively, significantly longer than typical W–O and W–F bonding distances found in other crystallographically characterized compounds.<sup>15</sup> Meanwhile, the neopentyl W–C–C angles of the two complexes are relatively wide at  $130.9(2)^\circ$  and  $129.7(2)^\circ$ , respectively, and are indicative of agostic interactions

(14) Bursten, B. E.; Cayton, R. H. *Organometallics* **1987**, *6*, 2004.

(15) A search of the Cambridge Structural Database reveals that W–F distances range from 1.657 to 2.189 Å with a mean distance of 1.924(0.110) Å and that W–O distances range from 1.689 to 2.400 Å with a mean distance of 1.973(0.108) Å.

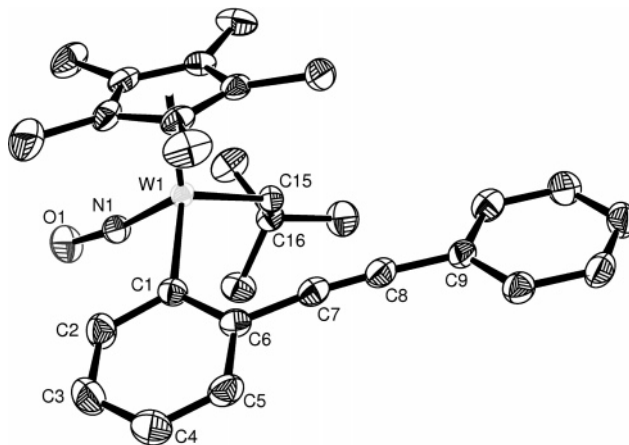


**Figure 4.** Solid-state molecular structure of  $\text{Cp}^*\text{W}(\text{NO})(\text{CH}_2\text{-CMe}_3)(o\text{-C}_6\text{H}_4\text{C}\equiv\text{CC}_6\text{H}_5)$  (**6a**) with 50% probability thermal ellipsoids shown. Selected interatomic distances (Å) and angles (deg):  $\text{W1-N1} = 1.767(3)$ ,  $\text{W1-C15} = 2.118(4)$ ,  $\text{W1-C1} = 2.156(4)$ ,  $\text{W1-C7} = 3.428$ ,  $\text{W1-C8} = 4.141$ ,  $\text{N1-O1} = 1.225(5)$ ,  $\text{W1-N1-O1} = 170.3(3)$ ,  $\text{W1-C15-C16} = 129.6(3)$ ,  $\text{W1-C1-C6} = 123.5(3)$ ,  $\text{C6-C7-C8} = 173.8(4)$ ,  $\text{C7-C8-C9} = 175.9(4)$ .

between the tungsten centers and a methylene proton on the neopentyl ligands.<sup>10</sup> Complexes containing halobenzene ligands bound to the metal centers via the halogens have been previously described in the literature.<sup>3b,16</sup> It is thus somewhat surprising that the electron-deficient metal centers in **2a** and **5a** interact with a C–H bond rather than the lone pairs on the F or O atoms in order to acquire additional electron density. Likewise, the C≡C bond in **6a** (Figure 4) does not interact with the W center, the W(1)–C(7) and W(1)–C(8) distances being 3.428 and 4.141 Å, respectively. The fact that the phenylethynyl group is bent away from W ( $\text{C}(6)\text{--C}(7)\text{--C}(8) = 173.8(4)^\circ$ ,  $\text{C}(7)\text{--C}(8)\text{--C}(9) = 176.0(4)^\circ$ ) is likely a manifestation of steric congestion around the metal center. Finally, in the solid-state molecular structure of complex **10c** (Figure 5), the fluorine trans to the nitrosyl group (i.e., F(1)) is closer to the W center than is the other fluorine (3.186 vs 3.398 Å), but these W–F distances are still too long for any bonding interactions to be considered.

**Preliminary Mechanistic Studies.** The lack of coordination of substituent lone pairs to tungsten in the C–H activated complexes, as evidenced by their NMR data and solid-state molecular structures, leads us to question whether precoordination of the substituted arenes via their heteroatoms to the metal centers is necessary for the subsequent C–H activations. Consequently, the early stages of the thermolysis of **1** in chlorobenzene have been monitored by <sup>1</sup>H NMR spectroscopy in order to acquire some mechanistic insights. Figure 6 shows the change in product ratios during the first 8 h of the thermolysis of **1** in chlorobenzene in a J. Young NMR tube at 70 °C. After just 1 h, the *o*:*m*:*p* ratio is 0.8:2:1, thereby indicating initial selectivity *against* the ortho isomer. However, the relative amount of the ortho isomer gradually increases throughout the 8 h period, while the amounts of the meta and para isomers show signs of leveling off.<sup>17</sup> These observations indicate that

(16) For examples of fluorobenzene complexes, see: (a) Bouwkamp, M. W.; Budzelaar, P. H. M.; Gercama, J.; Del Hierro Morales, I.; de Wolf, J.; Meetsma, A.; Troyanov, S. I.; Teuben, J. H.; Hessen, B. *J. Am. Chem. Soc.* **2005**, *127*, 14310, and references therein. (b) Basuli, F.; Aneetha, H.; Huffman, J. C.; Mindiola, D. J. *J. Am. Chem. Soc.* **2005**, *127*, 17992.

(17) Previous work in our group has shown that  $\text{Cp}^*\text{W}(\text{NO})(\text{CH}_2\text{CMe}_3)(o\text{-tolyl})$  isomerizes in  $\text{C}_6\text{D}_6$  at 70 °C over 2 days to a thermodynamic mixture having an *o*:*m*:*p* ratio of 1:59:40, identical to the aryl C–H activation product ratio resulting from the thermolysis of **1** in toluene.<sup>18</sup>

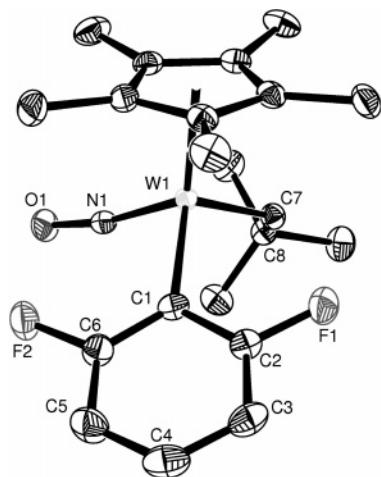


**Figure 5.** Solid-state molecular structure of  $\text{Cp}^*\text{W}(\text{NO})(\text{CH}_2\text{CMe}_3)(o\text{-C}_6\text{H}_3\text{F}_2)$  (**10c**) with 50% probability thermal ellipsoids shown. Selected interatomic distances ( $\text{\AA}$ ) and angles (deg):  $\text{W1-N1} = 1.7686(14)$ ,  $\text{W1-C7} = 2.1002(17)$ ,  $\text{W1-C1} = 2.1657(17)$ ,  $\text{W1-F1} = 3.186$ ,  $\text{W1-F2} = 3.398$ ,  $\text{N1-O1} = 1.2280(19)$ ,  $\text{W1-N1-O1} = 169.27(13)$ ,  $\text{W1-C7-C8} = 131.50(12)$ ,  $\text{W1-C1-C2} = 120.79(13)$ ,  $\text{W1-C1-C6} = 127.40(13)$ .

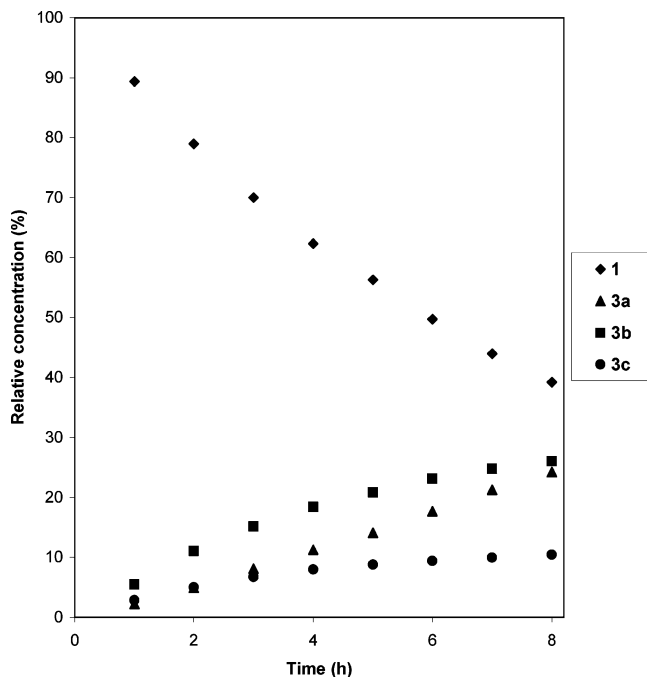


**Figure 6.** Relative amounts of the three isomers of  $\text{Cp}^*\text{W}(\text{NO})(\text{CH}_2\text{CMe}_3)(\text{C}_6\text{H}_4\text{Cl})$  (**3a-c**) during the first 8 h of thermolysis of  $\text{Cp}^*\text{W}(\text{NO})(\text{CH}_2\text{CMe}_3)_2$  (**1**) in chlorobenzene.

the selectivity of the alkylidene intermediate **A** for forming the ortho-activated isomer is thermodynamic rather than kinetic in nature. The meta and para isomers are formed first kinetically by activations of the most accessible C–H bonds,<sup>7</sup> and they then undergo conversion to the thermodynamically more stable ortho form. In these kinetic and thermodynamic aspects this system resembles Goldman's (PCP)Ir-based system, which also selectively generates chelated ortho-activated acetophenone and nitrobenzene complexes via intramolecular isomerizations.<sup>2b</sup>

Our ortho-selective C–H activations involve a combination of *both* steric and electronic factors. The decreasing ortho-selectivity (i.e.,  $\text{F} > \text{OMe} > \text{Cl} > \text{Br} > \text{C}\equiv\text{CPh}$ ) does correlate with increasing substituent size, but this cannot be the only factor operative since the corresponding  $\text{CH}_3$ -substituted phenyl

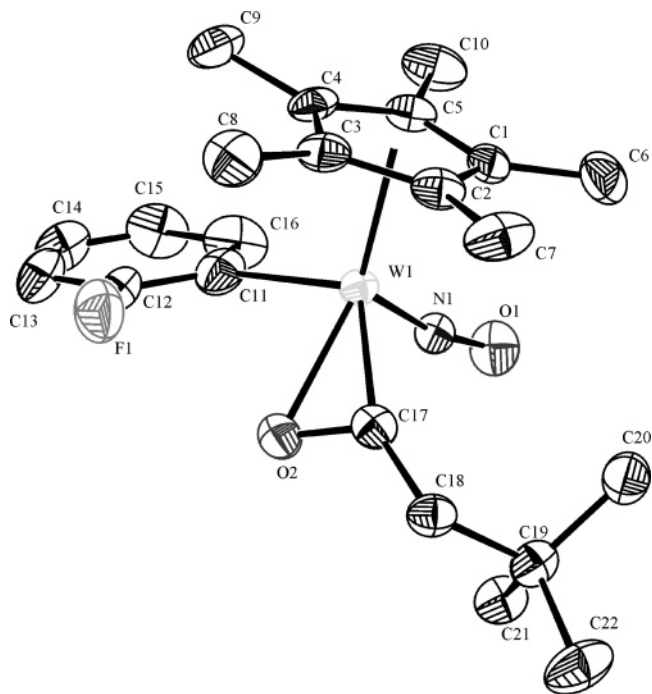


**Figure 7.** Solid-state molecular structure of  $\text{Cp}^*\text{W}(\text{NO})(\eta^2\text{-C(=O)CH}_2\text{CMe}_3)(o\text{-C}_6\text{H}_4\text{F})$  (**16**) with 50% probability thermal ellipsoids and hydrogen atoms having been omitted for clarity. Selected interatomic distances ( $\text{\AA}$ ) and angles (deg):  $\text{W1-N1} = 1.788(4)$ ,  $\text{W1-C17} = 2.067(4)$ ,  $\text{W1-C11} = 2.211(9)$ ,  $\text{W1-O2} = 2.219(3)$ ,  $\text{N1-O1} = 1.233(5)$ ,  $\text{C17-O2} = 1.248(5)$ ,  $\text{C17-C18} = 1.504(6)$ ,  $\text{W1-N1-O1} = 168.4(3)$ ,  $\text{W1-C11-C12} = 120.4(5)$ ,  $\text{W1-C17-C18} = 157.3(4)$ ,  $\text{W1-C17-O2} = 79.9(3)$ ,  $\text{W1-O2-C17} = 66.5(2)$ ,  $\text{C17-W1-N1} = 95.05(17)$ .

complexes do not undergo a similar conversion to the ortho isomer during the C–H activation of toluene.<sup>7,17</sup> Hence, the electron-withdrawing and -donating properties of the substituents must also influence the outcomes of these transformations even though no straightforward correlation is immediately evident. Clearly, more work is required to establish definitively how the ortho isomers are formed and why they are the thermodynamically most stable entities in these systems. At present we can only note that the isomerizations evidently do not involve reformation of alkylidene intermediate **A** since no crossover occurs when products **3a-c** are heated in benzene.

#### Representative Reactivity of C–H Activated Complex **2a**.

Unlike other halobenzene–C–H activating systems, the tungsten alkylidene complex **A** forms C–H activated compounds that are coordinatively and electronically unsaturated. As a result, they react readily with Lewis bases. For example, treatment of complex **2a** with tetraethylammonium cyanide ( $\text{Et}_4\text{NCN}$ ) and CO produces  $[\text{Et}_4\text{N}]^+[\text{Cp}^*\text{W}(\text{NO})(\text{CH}_2\text{CMe}_3)(\text{CN})(o\text{-C}_6\text{H}_4\text{F})]^-$  ( $[\text{Et}_4\text{N}]^+[\mathbf{15}]^-$ ) and  $\text{Cp}^*\text{W}(\text{NO})(\eta^2\text{-C(=O)CH}_2\text{CMe}_3)(o\text{-C}_6\text{H}_4\text{F})$  (**16**), respectively. By analogy to related systems, complex **16** is probably formed by initial coordination of CO to the metal center followed by its migratory insertion into the W– $\text{CH}_2\text{-CMe}_3$  linkage.<sup>19,20</sup> The identities of both complexes have been confirmed by conventional spectroscopic methods, and the solid-state molecular structure of 18-valence-electron **16** (Figure 7)

(18) Adams, C. S. Ph.D. Dissertation, University of British Columbia, 2001.

(19) Dryden, N. H.; Legzdins, P.; Lundmark, P. J.; Riesen, A.; Einstein, F. W. B. *Organometallics* **1993**, *12*, 2085.

(20) Debad, J. D.; Legzdins, P.; Batchelor, R. J.; Einstein, F. W. B. *Organometallics* **1993**, *12*, 2094.

has been established by a single-crystal X-ray crystallographic analysis.

## Epilogue

We have demonstrated that the C–H activating abilities of the 16-electron tungsten alkylidene intermediate  $\text{Cp}^*\text{W}(\text{NO})(=\text{CHCMe}_3)$  (**A**) are not hampered by Lewis-basic substituents on benzenes. Hence, **A** can be employed to activate ortho C–H bonds of halobenzenes (especially fluorobenzenes) and methoxybenzenes with good selectivity, an important first step in the utilization of  $\text{Cp}^*\text{W}(\text{NO})$ -based complexes in organic synthesis. The ortho-directing ability of the benzene functional groups decreases in the order  $\text{F} > \text{OMe} > \text{Cl} > \text{Br} > \text{C}\equiv\text{CPh}$ , and to the best of our knowledge, their ability to do so without coordination to the metal center is without precedent. We have also established that the ortho-selectivity is thermodynamic in nature, a feature exhibited by a few other C–H activating systems,<sup>2a,b</sup> and it reflects a juxtaposition of steric and electronic effects imparted by the substituents. The fact that the organometallic complexes formed by the C–H activations are both electronically and coordinatively unsaturated suggests that they should exhibit some interesting and useful derivatization chemistry. Studies designed to functionalize and release the activated organic fragments from the metal centers in a well-defined and productive manner are currently in progress.

## Experimental Section

**General Methods.** All reactions and subsequent manipulations involving organometallic reagents were performed under anaerobic and anhydrous conditions either at a vacuum-nitrogen dual manifold or in an inert-atmosphere drybox. General procedures routinely employed in these laboratories have been described in detail elsewhere.<sup>21,22</sup> Hexamethyldisiloxane (HMDS), pentane, hexanes, benzene-*d*<sub>6</sub>, diethyl ether, and tetrahydrofuran (THF) were all dried over sodium/benzophenone ketyl and were freshly distilled prior to use. Haloarenes, methoxyhaloarenes, anisole, and nitromethane were all purchased from Aldrich and were dried over, distilled from, and stored over  $\text{CaH}_2$  in resealable glass vessels. Acetone-*d*<sub>6</sub> was dried over and distilled from Drierite and was stored over 4 Å molecular sieves in a resealable glass vessel. Diphenylacetylene was recrystallized from ethanol and dried in vacuo prior to use.  $\text{Cp}^*\text{W}(\text{NO})(\text{CH}_2\text{CMe}_3)_2$  (**1**) was prepared according to the published procedure, but the compound was recrystallized in several batches from HMDS instead of pentane in order to maximize the amount of isolated product.<sup>6</sup> All other chemicals were purchased from Aldrich and were used as received. Unless specified otherwise, recrystallizations of newly synthesized complexes were effected overnight at  $-30$  °C.

All IR samples were prepared as Nujol mulls sandwiched between NaCl plates, and their spectra were recorded on a Thermo Nicolet Model 4700 FT-IR spectrometer. NMR spectra were recorded at room temperature on Bruker AV-300 or AV-400 instruments, and all chemical shifts and coupling constants are reported in ppm and in hertz, respectively.  $^1\text{H}$  NMR spectra were referenced to the residual protio isotopomer present in  $\text{C}_6\text{D}_6$  (7.16 ppm) or acetone-*d*<sub>6</sub> (2.04 ppm).  $^{13}\text{C}$  NMR spectra were referenced to  $\text{C}_6\text{D}_6$  (128 ppm), and  $^{19}\text{F}$  NMR spectra were referenced internally to  $\text{CF}_3\text{COOH}$  (0 ppm). Elemental and EI-MS analyses of the new complexes were performed by Mr. M. Lakha and Mr. M. Lapawa, respectively, in the Department of Chemistry at UBC.

(21) Lee, K.; Legzdins, P.; Pamplin, C. B.; Patrick, B. O.; Wada, K. *Organometallics* **2005**, *24*, 638.

(22) Legzdins, P.; Rettig, S. J.; Ross, K. J.; Batchelor, R. J.; Einstein, F. W. B. *Organometallics* **1995**, *14*, 5579.

**Representative Procedure for Effecting Preparative Thermolyses of 1 in Organic Substrates.** Unless noted otherwise, the following general procedure was used to prepare new compounds via thermolysis of **1**. A thick-walled, resealable vessel was charged with the specified amount of **1**, a magnetic stir bar, and approximately 2–3 mL of the organic substrate. The reaction mixture was subjected to three freeze–pump–thaw cycles before it was heated for 40 h at 70 °C in an oil bath. The volatile organics were then removed in vacuo, and the dried residue was redissolved in  $\text{C}_6\text{D}_6$  and was analyzed by IR and NMR spectroscopy. The NMR solvent was removed under reduced pressure, and the crude product was worked up as described in the following paragraphs. Reported yields are not optimized. Minor organometallic products that could not be isolated were characterized by their signals in the aryl region of the  $^1\text{H}$  NMR spectrum of the final reaction mixture. In addition, average product ratios were established by integration of appropriate signals in this spectrum, usually the upfield neopentyl methylene proton resonances, or in a few cases the downfield methylene proton resonances when the former signals were inadequately resolved. 1D selective COSY NMR experiments were performed on occasion to locate the aryl proton resonances of some minor products.

**$\text{Cp}^*\text{W}(\text{NO})(\text{CH}_2\text{CMe}_3)(\text{C}_6\text{H}_4\text{F})$  (**2a–c**).** The three complexes **2a–c** were prepared in a ratio of 97:2:1 via thermolysis of **1** (100.0 mg, 0.204 mmol) in fluorobenzene. Complex **2a** (80 mg, 77%) was obtained as dark red square plates by crystallization of the crude product mixture from HMDS in three crops.

**2a:** IR ( $\text{cm}^{-1}$ ):  $\nu(\text{NO})$  1592 (s).  $^1\text{H}$  NMR (400 MHz,  $\text{C}_6\text{D}_6$ ):  $\delta$   $-2.96$  (dd,  $^2J_{\text{HH}} = 11.0$  Hz,  $^5J_{\text{HF}} = 6.0$  Hz, 1H,  $\text{CH}_{\text{syn}}\text{H}$ ),  $1.25$  (s, 9H,  $\text{CMe}_3$ ),  $1.62$  (s, 15H,  $\text{C}_5\text{Me}_5$ ),  $5.46$  (d,  $^2J_{\text{HH}} = 11.0$  Hz, 1H,  $\text{CH}_{\text{anti}}\text{H}$ ),  $6.87$  (m, 1H, Ar H),  $6.97$  (overlapping m, 2H, Ar H),  $8.32$  (m, 1H, Ar H).  $^{19}\text{F}\{^1\text{H}\}$  NMR (282 MHz,  $\text{C}_6\text{D}_6$ ):  $\delta$   $-5.6$ . MS (LREI, *m/z*, probe temperature 100 °C): 515 [ $\text{M}^+$ ], 458 [ $\text{M}^+ - \text{CMe}_3$ ], 444 [ $\text{M}^+ - \text{CH}_2\text{CMe}_3$ ]. Anal. Calcd for  $\text{C}_{21}\text{H}_{30}\text{FNOW}$ : C 48.95, H 5.87, N 2.72. Found: C 48.83, H 5.80, N 2.63.

**2b:**  $^1\text{H}$  NMR (400 MHz,  $\text{C}_6\text{D}_6$ ):  $\delta$   $-2.34$  (d,  $^2J_{\text{HH}} = 11.0$  Hz, 1H,  $\text{CH}_{\text{syn}}\text{H}$ ),  $1.48$  (s, 15H,  $\text{C}_5\text{Me}_5$ ),  $4.78$  (d,  $^2J_{\text{HH}} = 11.0$  Hz, 1H,  $\text{CH}_{\text{anti}}\text{H}$ ),  $6.75$  (m, 1H, Ar H),  $7.04$  (m, 1H, Ar H),  $7.43$  (m, 1H, Ar H),  $7.54$  (m, 1H, Ar H). The signal due to the neopentyl methyl proton was probably obscured by the corresponding signal of **2a**.

**2c:**  $^1\text{H}$  NMR (400 MHz,  $\text{C}_6\text{D}_6$ ):  $\delta$   $-2.16$  (d,  $^2J_{\text{HH}} = 11.0$  Hz, 1H,  $\text{CH}_{\text{syn}}\text{H}$ ),  $1.50$  (s, 15H,  $\text{C}_5\text{Me}_5$ ),  $4.50$  (d,  $^2J_{\text{HH}} = 11.0$  Hz, 1H,  $\text{CH}_{\text{anti}}\text{H}$ ),  $7.59$  (m, 2H, Ar H). Again, the signal due to the neopentyl methyl proton of this complex was probably obscured by the corresponding signal of **2a**. The remaining aryl proton signal expected for this complex was also obscured.

**$\text{Cp}^*\text{W}(\text{NO})(\text{CH}_2\text{CMe}_3)(\text{C}_6\text{H}_4\text{Cl})$  (**3a–c**).** Complexes **3a–c** were prepared in a ratio of 75:17:8 via thermolysis of **1** (100.0 mg, 0.204 mmol) in chlorobenzene. The dried final product mixture was redissolved in a minimum of pentane and was transferred to the top of a column (1 × 3 cm) of neutral activated alumina I made up in pentane and supported on a medium-porosity frit. A red band containing **3a** was eluted from the column with 1:1 ether/pentane, while complexes **3b** and **3c** apparently decomposed on the column. The solvent was removed from the eluate in vacuo to obtain a red microcrystalline residue. Dark red rods of **3a** (65 mg, 60%) were obtained by recrystallization of this residue from 1:1 pentane/HMDS in two crops.

**3a:** IR ( $\text{cm}^{-1}$ ):  $\nu(\text{NO})$  1589 (s).  $^1\text{H}$  NMR (400 MHz,  $\text{C}_6\text{D}_6$ ):  $\delta$   $-2.48$  (d,  $^2J_{\text{HH}} = 11.0$  Hz, 1H,  $\text{CH}_{\text{syn}}\text{H}$ ),  $1.28$  (s, 9H,  $\text{CMe}_3$ ),  $1.61$  (s, 15H,  $\text{C}_5\text{Me}_5$ ),  $5.43$  (d,  $^2J_{\text{HH}} = 11.0$  Hz, 1H,  $\text{CH}_{\text{anti}}\text{H}$ ),  $6.84$  (ddd, 1H, Ar H),  $6.98$  (ddd, 1H, Ar H),  $7.26$  (dd,  $^3J_{\text{HH}} = 7.9$  Hz,  $^4J_{\text{HH}} = 0.8$  Hz, 1H, Ar H),  $8.26$  (br d,  $^3J_{\text{HH}} = 6.2$  Hz, 1H, Ar H).  $^{13}\text{C}\{^1\text{H}\}$  NMR (100 MHz,  $\text{C}_6\text{D}_6$ ):  $\delta$   $9.5$  ( $\text{C}_5\text{Me}_5$ ),  $33.2$  ( $\text{CH}_2\text{CMe}_3$ ),  $41.8$  ( $\text{CH}_2\text{CMe}_3$ ),  $110.6$  ( $\text{C}_5\text{Me}_5$ ),  $125.8$  (Ar C),  $128.3$  (Ar C),  $128.6$  (Ar C),  $135.8$  ( $\text{CH}_2\text{CMe}_3$ ),  $138.7$  ( $\text{C}_{\text{C}_{\text{ipso}}}$ ),  $141.7$  (Ar C),  $178.2$  ( $\text{WC}_{\text{ipso}}$ ). MS (LREI, *m/z*, probe temperature 100 °C): 531 [ $\text{M}^+$ ], 474 [ $\text{M}^+$

– CMe<sub>3</sub>], 460 [M<sup>+</sup> – CH<sub>2</sub>CMe<sub>3</sub>]. Anal. Calcd for C<sub>21</sub>H<sub>30</sub>ClNOW: C 47.43, H 6.09, N 2.63. Found: C 47.33, H 6.10, N 2.53.

**3b**: <sup>1</sup>H NMR (400 MHz, C<sub>6</sub>D<sub>6</sub>): δ –2.43 (d, <sup>2</sup>J<sub>HH</sub> = 11.0 Hz, 1H, CH<sub>syn</sub>H), 1.23 (s, 9H, CMe<sub>3</sub>), 1.47 (s, 15H, C<sub>5</sub>Me<sub>5</sub>), 4.82 (d, <sup>2</sup>J<sub>HH</sub> = 11.0 Hz, 1H, CH<sub>anti</sub>H), 6.93 (t, 1H, Ar H), 7.07 (m, 1H, Ar H), 7.58 (d, 1H, Ar H), 7.78 (br s, 1H, Ar H).

**3c**: <sup>1</sup>H NMR (400 MHz, C<sub>6</sub>D<sub>6</sub>): δ –2.31 (d, <sup>2</sup>J<sub>HH</sub> = 11.0 Hz, 1H, CH<sub>syn</sub>H), 1.26 (s, 9H, CMe<sub>3</sub>), 1.48 (s, 15H, C<sub>5</sub>Me<sub>5</sub>), 4.64 (d, <sup>2</sup>J<sub>HH</sub> = 11.0 Hz, 1H, CH<sub>anti</sub>H), 7.17 (obscured, 2H, Ar H), 7.50 (d, <sup>3</sup>J<sub>HH</sub> = 8.0 Hz, 2H, Ar H).

**Cp\*W(NO)(CH<sub>2</sub>CMe<sub>3</sub>)(C<sub>6</sub>H<sub>4</sub>Br) (4a–c)**. This reaction was performed and worked up in a manner identical to that described in the preceding section for the thermolysis of **1** in chlorobenzene. Complex **4a** was isolated as dark red rods (57 mg, 46%) by crystallization of the chromatographed product from 1:1 pentane/HMDS solutions in three crops.

**4a**: IR (cm<sup>–1</sup>): ν(NO) 1596 (s). <sup>1</sup>H NMR (400 MHz, C<sub>6</sub>D<sub>6</sub>): δ –2.01 (br, 1H, CH<sub>syn</sub>H), 1.28 (s, 9H, CMe<sub>3</sub>), 1.63 (s, 15H, C<sub>5</sub>Me<sub>5</sub>), 5.37 (d, <sup>2</sup>J<sub>HH</sub> = 10.8 Hz, 1H, CH<sub>anti</sub>H), 6.72 (ddd, 1H, Ar H), 7.00 (ddd, 1H, Ar H), 7.48 (dd, <sup>3</sup>J<sub>HH</sub> = 7.8 Hz, <sup>4</sup>J<sub>HH</sub> = 1.0 Hz, 1H, Ar H), 8.21 (br d, 1H, Ar H). <sup>13</sup>C{<sup>1</sup>H} (100 MHz, C<sub>6</sub>D<sub>6</sub>): δ 10.1 (C<sub>5</sub>Me<sub>5</sub>), 33.7 (CH<sub>2</sub>CMe<sub>3</sub>), 42.3 (CH<sub>2</sub>CMe<sub>3</sub>), 111.0 (C<sub>5</sub>Me<sub>5</sub>), 113.0 (Ar C), 126.4 (Ar C), 129.0 (Ar C), 132.0, 132.0, 136.0 (CH<sub>2</sub>CMe<sub>3</sub>), 142.7 (Ar C), 182.7 (WC<sub>ipso</sub>). MS (LREI, *m/z*, probe temperature 100 °C): 575 [M<sup>+</sup>], 518 [M<sup>+</sup> – CMe<sub>3</sub>]. Anal. Calcd for C<sub>21</sub>H<sub>30</sub>BrNOW: C 43.77, H 5.25, N 2.43. Found: C 43.83, H 5.11, N 2.57.

**4b**: <sup>1</sup>H NMR (400 MHz, C<sub>6</sub>D<sub>6</sub>): δ –2.46 (d, <sup>2</sup>J<sub>HH</sub> = 11.2 Hz, 1H, CH<sub>syn</sub>H), 1.21 (s, 9H, CMe<sub>3</sub>), 1.48 (s, 15H, C<sub>5</sub>Me<sub>5</sub>), 4.83 (d, <sup>2</sup>J<sub>HH</sub> = 11.2 Hz, 1H, CH<sub>anti</sub>H), 6.87 (t, 1H, Ar H), 7.20 (m, 1H, Ar H), 7.64 (d, 1H, Ar H), 7.91 (s, 1H, Ar H).

**4c**: <sup>1</sup>H NMR (400 MHz, C<sub>6</sub>D<sub>6</sub>): δ –2.36 (d, <sup>2</sup>J<sub>HH</sub> = 11.2 Hz, 1H, CH<sub>syn</sub>H), 1.25 (s, 9H, CMe<sub>3</sub>), 1.49 (s, 15H, C<sub>5</sub>Me<sub>5</sub>), 4.68 (d, <sup>2</sup>J<sub>HH</sub> = 11.2 Hz, 1H, CH<sub>anti</sub>H), 7.31 (d, <sup>3</sup>J<sub>HH</sub> = 8.0 Hz, 2H, Ar H), 7.42 (d, <sup>3</sup>J<sub>HH</sub> = 8.0 Hz, 2H, Ar H).

**Cp\*W(NO)(CH<sub>2</sub>CMe<sub>3</sub>)(C<sub>6</sub>H<sub>4</sub>OMe) (5a–c)**. Complexes **5a–c** were prepared via thermolysis of **1** (90.0 mg, 0.183 mmol) in anisole. Complex **5a** (72 mg, 70%) was obtained as purple diamond-shaped plates by crystallization of the final product mixture from an ether/HMDS bilayer in three crops.

**5a**: IR (cm<sup>–1</sup>): ν(NO) 1564 (s). <sup>1</sup>H NMR (400 MHz, C<sub>6</sub>D<sub>6</sub>): δ –2.66 (d, <sup>2</sup>J<sub>HH</sub> = 11.8 Hz, 1H, CH<sub>syn</sub>H), 1.33 (s, 9H, CMe<sub>3</sub>), 1.62 (s, 15H, C<sub>5</sub>Me<sub>5</sub>), 3.14 (s, 3H, OMe), 4.90 (d, <sup>2</sup>J<sub>HH</sub> = 11.8 Hz, 1H, CH<sub>anti</sub>H), 6.54 (ddd, 1H, Ar H), 6.97 (ddd, 1H, Ar H), 7.14 (dd, <sup>3</sup>J<sub>HH</sub> = 7.9 Hz, <sup>4</sup>J<sub>HH</sub> = 0.8 Hz, 1H, Ar H), 8.47 (dd, <sup>3</sup>J<sub>HH</sub> = 8.0 Hz, <sup>4</sup>J<sub>HH</sub> = 0.8 Hz, 1H, Ar H). <sup>13</sup>C{<sup>1</sup>H} (100 MHz, C<sub>6</sub>D<sub>6</sub>): δ 9.9 (C<sub>5</sub>Me<sub>5</sub>), 33.9 (CH<sub>2</sub>CMe<sub>3</sub>), 41.0 (CH<sub>2</sub>CMe<sub>3</sub>), 54.1 (OMe), 109.3 (Ar C), 110.6 (C<sub>5</sub>Me<sub>5</sub>), 121.8 (Ar C), 129.2 (CH<sub>2</sub>CMe<sub>3</sub>), 141.3 (Ar C), 135.8 (CH<sub>2</sub>CMe<sub>3</sub>), 160.0 (MeOC<sub>ipso</sub>), 169.3 (WC<sub>ipso</sub>). MS (LREI, *m/z*, probe temperature 100 °C): 527 [M<sup>+</sup>], 470 [M<sup>+</sup> – CMe<sub>3</sub>]. Anal. Calcd for C<sub>22</sub>H<sub>33</sub>NO<sub>2</sub>W: C 50.11, H 6.31, N 2.66. Found: C 50.33, H 6.17, N 2.73.

**5b**: <sup>1</sup>H NMR (400 MHz, C<sub>6</sub>D<sub>6</sub>): δ –2.43 (d, <sup>2</sup>J<sub>HH</sub> = 11.0 Hz, 1H, CH<sub>syn</sub>H), 1.23 (s, 9H, CMe<sub>3</sub>), 1.47 (s, 15H, C<sub>5</sub>Me<sub>5</sub>), 4.82 (d, <sup>2</sup>J<sub>HH</sub> = 11.0 Hz, 1H, CH<sub>anti</sub>H), 6.93 (t, 1H, Ar H), 7.07 (m, 1H, Ar H), 7.58 (d, 1H, Ar H), 7.78 (br s, 1H, Ar H).

**5c**: <sup>1</sup>H NMR (400 MHz, C<sub>6</sub>D<sub>6</sub>): δ –2.31 (d, <sup>2</sup>J<sub>HH</sub> = 11.0 Hz, 1H, CH<sub>syn</sub>H), 1.26 (s, 9H, CMe<sub>3</sub>), 1.48 (s, 15H, C<sub>5</sub>Me<sub>5</sub>), 4.64 (d, <sup>2</sup>J<sub>HH</sub> = 11.0 Hz, 1H, CH<sub>anti</sub>H), 7.17 (obscured, 2H, Ar H), 7.50 (d, <sup>3</sup>J<sub>HH</sub> = 8.0 Hz, 2H, Ar H).

**Cp\*W(NO)(CH<sub>2</sub>CMe<sub>3</sub>)(*o*-C<sub>6</sub>H<sub>4</sub>C≡CC<sub>6</sub>H<sub>5</sub>) (6a) and Cp\*W(NO)(η<sup>3</sup>,η<sup>1</sup>-(CMe<sub>3</sub>)HCCPh=CPh–CPh=CPh) (6d)**. A resealable vessel was charged with **1** (89.0 mg, 0.181 mmol), diphenylacetylene (400.0 mg, 2.24 mmol), and a magnetic stir bar. The vessel was evacuated before being heated in a 70 °C oil bath for 40 h. The volatiles were removed from the final reaction mixture in vacuo, and the remaining residue was dissolved in a minimum amount of

pentane. The pentane solution was transferred to the top of a column (2 × 8 cm) of neutral activated alumina I made up in pentane and supported on a medium-porosity frit. The column was washed with pentane (~300 mL) until no white residue (diphenylacetylene) formed when a drop of the eluate was allowed to evaporate. The column was then eluted with 1:4 ether/pentane, whereupon an orange band eluted ahead of a red band. The orange band was collected, and the solvent was removed from it in vacuo. Compound **6d** (4 mg, 3% based on tungsten) was obtained as orange irregularly shaped plates by recrystallization of the orange residue from pentane. Because of the low yield, only IR and <sup>1</sup>H NMR data were obtained for this compound.

After the orange band had been collected, the eluant composition was changed to 1:1 ether/pentane. The red band was next eluted and collected, and the eluate was taken to dryness in vacuo to obtain a red-brown residue. This residue was washed with cold pentane (3 × 5 mL) and was redissolved in a minimum of diethyl ether. Pentane was carefully layered on top of this solution, and storage of this mixture overnight in a freezer at –30 °C resulted in the deposition of dark purple diamond-shaped crystals of **6a** (45 mg, 42%).

**6a**: IR (cm<sup>–1</sup>): ν(NO) 1568 (s). <sup>1</sup>H NMR (400 MHz, C<sub>6</sub>D<sub>6</sub>): δ –2.24 (br d, <sup>2</sup>J<sub>HH</sub> = 10.6 Hz, 1H, CH<sub>syn</sub>H), 1.33 (s, 9H, CMe<sub>3</sub>), 1.61 (s, 15H, C<sub>5</sub>Me<sub>5</sub>), 5.59 (d, <sup>2</sup>J<sub>HH</sub> = 11.0 Hz, 1H, CH<sub>anti</sub>H), 6.95–7.13 (m, 5H, Ar H), 7.51 (br d, 2H, Ar H), 7.67 (br d, 1H, Ar H), 8.34 (br d, 1H, Ar H). <sup>13</sup>C{<sup>1</sup>H} NMR (100 MHz, C<sub>6</sub>D<sub>6</sub>): δ 10.1 (C<sub>5</sub>Me<sub>5</sub>), 33.7 (CH<sub>2</sub>CMe<sub>3</sub>), 42.4 (CH<sub>2</sub>CMe<sub>3</sub>), 95.0 (C≡C), 95.9 (C≡C), 110.9 (C<sub>5</sub>Me<sub>5</sub>), 126.9 (Ar C), 128.6 (Ar C), 131.7 (Ar C), 133.4 (Ar C), 137.9 (CH<sub>2</sub>CMe<sub>3</sub>), 140.6 (Ar C), 185.6 (WC<sub>ipso</sub>). Other aryl carbon signals are probably obscured by the C<sub>6</sub>D<sub>6</sub> signal. MS (LREI, *m/z*, probe temperature 100 °C): 597 [M<sup>+</sup>], 540 [M<sup>+</sup> – CMe<sub>3</sub>], 526 [M<sup>+</sup> – CH<sub>2</sub>CMe<sub>3</sub>]. Anal. Calcd for C<sub>29</sub>H<sub>35</sub>NO: C 58.30, H 5.91, N 2.34. Found: C 58.31, H 5.82, N 2.53.

**6d**: IR (cm<sup>–1</sup>): ν(NO) 1563 (s). <sup>1</sup>H NMR (400 MHz, C<sub>6</sub>D<sub>6</sub>): δ 1.21 (s, 9H, CMe<sub>3</sub>), 1.39 (s, 15H, C<sub>5</sub>Me<sub>5</sub>), 3.76 (s, Me<sub>3</sub>CCH), 6.60–8.39 (m, 20H, Ar H).

**Cp\*W(NO)(η<sup>3</sup>,η<sup>1</sup>-(Me<sub>3</sub>C)HC–CEt=CEt–CEt=CEt) (7)**. Complex **7** was the only identifiable organometallic product formed during the thermolysis of **1** (98 mg, 2.0 mmol) in 3-hexyne. The final product mixture was taken to dryness, the residue was redissolved in a minimum of pentane, and this solution was transferred to the top of a neutral, activated alumina I column (1 × 3 cm) supported on a medium-porosity frit. Elution of the column with 1:5 ether/pentane led to the development of an orange band, which was collected. The solvents were removed from the eluate in vacuo, and the residue was redissolved in a minimum of pentane. This pentane solution was stored overnight at –30 °C to induce the deposition of orange rectangular prisms of **7** (25 mg, 22% yield).

**7**: IR (cm<sup>–1</sup>): ν(NO) 1583 (s). <sup>1</sup>H NMR (400 MHz, C<sub>6</sub>D<sub>6</sub>): δ 1.10 (t, 3H, CH<sub>2</sub>CH<sub>3</sub>), 1.12 (t, 3H, CH<sub>2</sub>CH<sub>3</sub>), 1.14 (t, 3H, CH<sub>2</sub>CH<sub>3</sub>), 1.32 (s, 9H, CMe<sub>3</sub>), 1.48 (m, 1H, CH<sub>2</sub>), 1.63 (m, 1H, CH<sub>2</sub>), 1.68 (s, 15H, C<sub>5</sub>Me<sub>5</sub>), 2.00 (m, 1H, CH<sub>2</sub>), 2.25 (m, 1H, CH<sub>2</sub>), 2.30 (m, 1H, CH<sub>2</sub>), 2.35 (s, 1H, allyl CH), 2.96 (m, 2H, CH<sub>2</sub>), 3.24 (m, 1H, CH<sub>2</sub>). <sup>13</sup>C{<sup>1</sup>H} NMR (100 MHz, C<sub>6</sub>D<sub>6</sub>): δ 10.5 (C<sub>5</sub>Me<sub>5</sub>), 13.9 (CH<sub>2</sub>CH<sub>3</sub>), 14.9 (CH<sub>2</sub>CH<sub>3</sub>), 20.0 (CH<sub>2</sub>CH<sub>3</sub>), 20.7 (CH<sub>2</sub>CH<sub>3</sub>), 26.6 (CH<sub>2</sub>CH<sub>3</sub>), 26.7 (CH<sub>2</sub>CH<sub>3</sub>), 28.0 (CH<sub>2</sub>CH<sub>3</sub>), 28.7 (CH<sub>2</sub>CH<sub>3</sub>), 34.4 (CH<sub>2</sub>CMe<sub>3</sub>), 36.6 82.1 (CH(CMe<sub>3</sub>)), 83.4 (allyl C), 106.3 (C<sub>5</sub>Me<sub>5</sub>), 130.6 (allyl C), 143.8 (vinyl C), 159.2 (vinyl C). MS (LREI, *m/z*, probe temperature 100 °C): 583 [M<sup>+</sup>]. Anal. Calcd for C<sub>27</sub>H<sub>45</sub>NO: C 55.58, H 7.77, N 2.40. Found: C 55.77, H 7.67, N 2.50.

**Cp\*W(NO)(CH<sub>2</sub>CMe<sub>3</sub>)(C<sub>6</sub>H<sub>3</sub>F<sub>2</sub>) (8a,b)**. Complexes **8a** and **8b** were prepared via thermolysis of **1** (100.0 mg, 0.204 mmol) in *o*-difluorobenzene. Complex **8a** was isolated as dark red, square plates (80 mg, 74%) by crystallization of the dried final product mixture from 1:1 pentane/HMDS in two crops.

**8a**: IR (cm<sup>–1</sup>): ν(NO) 1596 (s). <sup>1</sup>H NMR (400 MHz, C<sub>6</sub>D<sub>6</sub>): δ –3.17 (dd, <sup>2</sup>J<sub>HH</sub> = 10.8 Hz, <sup>5</sup>J<sub>HF</sub> = 6.2 Hz, 1H, CH<sub>syn</sub>H), 1.22 (s,



9H, CMe<sub>3</sub>), 1.57 (s, 15H, C<sub>5</sub>Me<sub>5</sub>), 5.66 (d, <sup>2</sup>J<sub>HH</sub> = 10.8 Hz, 1H, CH<sub>anti</sub>H), 6.44 (m, 2H, Ar H), 7.88 (m, 1H, Ar H). <sup>19</sup>F{<sup>1</sup>H} NMR (282 MHz, C<sub>6</sub>D<sub>6</sub>): δ -33.3, -62.1. MS (LREI, *m/z*, probe temperature 100 °C): 533 [M<sup>+</sup>], 476 [M<sup>+</sup> - CMe<sub>3</sub>]. Anal. Calcd for C<sub>21</sub>H<sub>29</sub>F<sub>2</sub>NOW: C 47.29, H 5.48, N 2.63. Found: C 47.44, H 5.80, N 2.67.

**8b**: <sup>1</sup>H NMR (400 MHz, C<sub>6</sub>D<sub>6</sub>): δ -2.46 (d, <sup>2</sup>J<sub>HH</sub> = 10.8 Hz, 1H, CH<sub>syn</sub>H), 1.46 (s, 15H, C<sub>5</sub>Me<sub>5</sub>), 4.77 (d, <sup>2</sup>J<sub>HH</sub> = 11.0 Hz, 1H, CH<sub>anti</sub>H), 7.22 (m, 1H, Ar H), 7.65 (m, 1H, Ar H). The neopentyl methyl proton signal and one aryl proton signal were probably obscured by the signals of **8a**.

**Cp\*W(NO)(CH<sub>2</sub>CMe<sub>3</sub>)(C<sub>6</sub>H<sub>3</sub>Cl<sub>2</sub>) (9a,b)**. Complexes **9a** and **9b** were prepared via thermolysis of **1** (91.0 mg, 0.185 mmol) in *o*-dichlorobenzene. At the end of the 40 h reaction period, the vessel was wrapped in aluminum foil, and *o*-dichlorobenzene (bp 180 °C) was removed in vacuo at 60 °C. The dried product mixture was redissolved in a minimum of pentane, and the pentane solution was transferred to the top of a neutral activated alumina I column (1 × 3 cm) made up in pentane and supported on a medium-porosity frit. The column was eluted with 1:1 ether/pentane, whereupon a red band developed. The band was eluted and collected, and the solvent was removed from the eluate to obtain a red microcrystalline powder. Compound **9a** was obtained as red plates (65 mg, 62%, 2 crops) by recrystallization of this powder from pentane.

**9a**: IR (cm<sup>-1</sup>): ν(NO) 1580 (s). <sup>1</sup>H NMR (400 MHz, C<sub>6</sub>D<sub>6</sub>): δ -2.46 (d, <sup>2</sup>J<sub>HH</sub> = 11.1 Hz, 1H, CH<sub>syn</sub>H), 1.32 (s, 9H, CMe<sub>3</sub>), 1.62 (s, 15H, C<sub>5</sub>Me<sub>5</sub>), 5.52 (d, <sup>2</sup>J<sub>HH</sub> = 11.1 Hz, 1H, CH<sub>anti</sub>H), 6.77 (t, 1H, <sup>3</sup>J<sub>HH</sub> = 7.9 Hz, Ar H), 7.06 (dd, <sup>3</sup>J<sub>HH</sub> = 7.9 Hz, <sup>4</sup>J<sub>HH</sub> = 1.0 Hz, 1H, Ar H), 8.04 (dd, <sup>3</sup>J<sub>HH</sub> = 7.9 Hz, <sup>4</sup>J<sub>HH</sub> = 1.0 Hz, 1H, Ar H). <sup>13</sup>C{<sup>1</sup>H} NMR (100 MHz, C<sub>6</sub>D<sub>6</sub>): δ 9.9 (C<sub>5</sub>Me<sub>5</sub>), 33.5 (CH<sub>2</sub>CMe<sub>3</sub>), 42.4 (CH<sub>2</sub>CMe<sub>3</sub>), 111.2 (C<sub>5</sub>Me<sub>5</sub>), 129.1 (Ar C), 130.8 (Ar C), 132.7 (Ar C), 133.4 (CH<sub>2</sub>CMe<sub>3</sub>), 139.9 (Ar C), 181.0 (WC<sub>ipso</sub>). Other aryl carbon signals were not observed. MS (LREI, *m/z*, probe temperature 100 °C): 565 [M<sup>+</sup>], 508 [M<sup>+</sup> - CMe<sub>3</sub>]. Anal. Calcd for C<sub>21</sub>H<sub>29</sub>Cl<sub>2</sub>NOW: C 44.54, H 5.16, N 2.47. Found: C 44.32, H 5.07, N 2.43.

**9b**: <sup>1</sup>H NMR (400 MHz, C<sub>6</sub>D<sub>6</sub>): δ -2.54 (d, <sup>2</sup>J<sub>HH</sub> = 11.1 Hz, 1H, CH<sub>syn</sub>H), 1.29 (s, 9H, CMe<sub>3</sub>), 1.51 (s, 15H, C<sub>5</sub>Me<sub>5</sub>), 4.98 (d, <sup>2</sup>J<sub>HH</sub> = 11.1 Hz, 1H, CH<sub>anti</sub>H), 6.95 (m, 1H, Ar H), 7.38 (m, 1H, Ar H), 7.80 (d, 1H, Ar H).

**Cp\*W(NO)(CH<sub>2</sub>CMe<sub>3</sub>)(C<sub>6</sub>H<sub>3</sub>F<sub>2</sub>) (10a,c)**. Complexes **10a** and **10c** were prepared via thermolysis of **1** (101 mg, 0.206 mmol) in *m*-difluorobenzene. The final dried product mixture was dissolved in a minimum of pentane, and the pentane solution was loaded onto a neutral activated alumina I column (2 × 7 cm) made up in pentane and supported on a medium-porosity frit. Elution of the column with 1:4 ether/pentane developed two resolvable bands, a red one containing **10a** that eluted ahead of the red-purple band containing **10c**. Once the resolution of the two bands was complete, the eluant composition was changed to 2:1 ether/pentane. The two bands were then eluted and collected separately, and the solvents were removed from the collected eluates in vacuo. The desired compounds were isolated by recrystallization of the residues from pentane/HMDS and HMDS, respectively, to obtain red irregularly shaped crystals of **10a** (64 mg, 59%) and dark red rods of **10c** (6 mg, 5%, 2 crops).

**10a**: IR (cm<sup>-1</sup>): ν(NO) 1595 (s). <sup>1</sup>H NMR (400 MHz, C<sub>6</sub>D<sub>6</sub>): δ -3.03 (dd, <sup>2</sup>J<sub>HH</sub> = 11.2 Hz, <sup>5</sup>J<sub>HF</sub> = 5.5 Hz, 1H, CH<sub>syn</sub>H), 1.25 (s, 9H, CMe<sub>3</sub>), 1.58 (s, 15H, C<sub>5</sub>Me<sub>5</sub>), 5.43 (d, <sup>2</sup>J<sub>HH</sub> = 11.2 Hz, 1H, CH<sub>anti</sub>H), 6.57 (m, 1H, Ar H), 6.67 (m, 1H, Ar H), 8.14 (m, 1H, Ar H). <sup>19</sup>F{<sup>1</sup>H} NMR (282 MHz, C<sub>6</sub>D<sub>6</sub>): δ -2.7, -34.2. MS (LREI, *m/z*, probe temperature 100 °C): 533 [M<sup>+</sup>], 476 [M<sup>+</sup> - CMe<sub>3</sub>], 462 [M<sup>+</sup> - CH<sub>2</sub>CMe<sub>3</sub>]. Anal. Calcd for C<sub>21</sub>H<sub>29</sub>F<sub>2</sub>NOW: C 47.29, H 5.48, N 2.63. Found: C 47.14, H 5.26, N 2.37.

**10c**: IR (cm<sup>-1</sup>): ν(NO) 1609 (s). <sup>1</sup>H NMR (400 MHz, C<sub>6</sub>D<sub>6</sub>): δ -2.97 (dt, <sup>2</sup>J<sub>HH</sub> = 10.9 Hz, <sup>5</sup>J<sub>HF</sub> = 3.7 Hz, CH<sub>syn</sub>H), 1.27 (s, 15H, C<sub>5</sub>Me<sub>5</sub>), 1.64 (s, 15H, C<sub>5</sub>Me<sub>5</sub>), 5.76 (d, <sup>2</sup>J<sub>HH</sub> = 10.9 Hz, 1H,

CH<sub>anti</sub>H), 6.65 (m, 1H, Ar H), 6.76 (m, 2H, Ar H). <sup>19</sup>F{<sup>1</sup>H} NMR (282 MHz, C<sub>6</sub>D<sub>6</sub>): δ -2.1. MS (LREI, *m/z*, probe temperature 100 °C): 533 [M<sup>+</sup>], 476 [M<sup>+</sup> - CMe<sub>3</sub>], 462 [M<sup>+</sup> - CH<sub>2</sub>CMe<sub>3</sub>].

**Cp\*W(NO)(CH<sub>2</sub>CMe<sub>3</sub>)(C<sub>6</sub>H<sub>3</sub>Cl<sub>2</sub>) (11a,b)**. This reaction involving *m*-dichlorobenzene was performed and worked up in a manner identical to that described above for the thermolysis of **1** in *o*-dichlorobenzene. Complex **11a** was isolated as red needles (67 mg, 54%, 2 crops) by crystallization of the chromatographed product from pentane.

**11a**: IR (cm<sup>-1</sup>): ν(NO) 1580 (s). <sup>1</sup>H NMR (400 MHz, C<sub>6</sub>D<sub>6</sub>): δ -2.63 (d, <sup>2</sup>J<sub>HH</sub> = 10.9 Hz, 1H, CH<sub>syn</sub>H), 1.27 (s, 9H, CMe<sub>3</sub>), 1.56 (s, 15H, C<sub>5</sub>Me<sub>5</sub>), 5.47 (d, <sup>2</sup>J<sub>HH</sub> = 10.9 Hz, 1H, CH<sub>anti</sub>H), 6.96 (dd, 1H, <sup>3</sup>J<sub>HH</sub> = 8.0 Hz, <sup>4</sup>J<sub>HH</sub> = 1.0 Hz, Ar H), 7.30 (d, <sup>4</sup>J<sub>HH</sub> = 1.0 Hz, 1H, Ar H), 8.02 (d, <sup>3</sup>J<sub>HH</sub> = 8.0 Hz, 1H, Ar H). <sup>13</sup>C{<sup>1</sup>H} (100 MHz, C<sub>6</sub>D<sub>6</sub>): δ 9.9 (C<sub>5</sub>Me<sub>5</sub>), 33.5 (CH<sub>2</sub>CMe<sub>3</sub>), 42.4 (CH<sub>2</sub>CMe<sub>3</sub>), 111.1 (C<sub>5</sub>Me<sub>5</sub>), 126.6 (Ar C), 128.5 (Ar C), 134.2 (CH<sub>2</sub>CMe<sub>3</sub>), 138.0 (Ar C), 139.8 (Ar C), 142.8 (Ar C), 176.3 (WC<sub>ipso</sub>). MS (LREI, *m/z*, probe temperature 100 °C): 565 [M<sup>+</sup>], 508 [M<sup>+</sup> - CMe<sub>3</sub>]. Anal. Calcd for C<sub>21</sub>H<sub>29</sub>Cl<sub>2</sub>NOW: C 44.54, H 5.16, N 2.47. Found: C 44.19, H 5.00, N 2.68.

**11b**: <sup>1</sup>H NMR (400 MHz, C<sub>6</sub>D<sub>6</sub>): δ -2.73 (d, <sup>2</sup>J<sub>HH</sub> = 11.1 Hz, 1H, CH<sub>syn</sub>H), 1.19 (s, 9H, CMe<sub>3</sub>), 1.42 (s, 15H, C<sub>5</sub>Me<sub>5</sub>), 5.08 (d, <sup>2</sup>J<sub>HH</sub> = 11.1 Hz, 1H, CH<sub>anti</sub>H), 7.08 (t, 1H, Ar H), 7.65 (s, 2H, Ar H).

**Cp\*W(NO)(CH<sub>2</sub>CMe<sub>3</sub>)(C<sub>6</sub>H<sub>3</sub>ClF) (12a,b)**. Complexes **12a** and **12b** were formed by the thermolysis of **1** (95.0 mg, 0.194 mmol) in *p*-chlorofluorobenzene. Complex **12a** (48 mg, 45%) was isolated analytically pure by crystallization of the crude product mixture from pentane in three crops. No attempts were made to isolate **12b**.

**12a**: IR (cm<sup>-1</sup>): ν(NO) 1599 (s). <sup>1</sup>H NMR (400 MHz, C<sub>6</sub>D<sub>6</sub>): δ -3.18 (dd, <sup>2</sup>J<sub>HH</sub> = 10.6 Hz, <sup>5</sup>J<sub>HF</sub> = 6.0 Hz, 1H, CH<sub>syn</sub>H), 1.22 (s, 9H, CMe<sub>3</sub>), 1.55 (s, 15H, C<sub>5</sub>Me<sub>5</sub>), 5.63 (d, <sup>2</sup>J<sub>HH</sub> = 10.6 Hz, 1H, CH<sub>anti</sub>H), 6.59 (m, 1H, Ar H), 6.92 (m, 1H, Ar H), 8.30 (m, 1H, Ar H). <sup>19</sup>F{<sup>1</sup>H} NMR (282 MHz, C<sub>6</sub>D<sub>6</sub>): δ -9.3. MS (LREI, *m/z*, probe temperature 100 °C): 549 [M<sup>+</sup>], 492 [M<sup>+</sup> - CMe<sub>3</sub>], 478 [M<sup>+</sup> - CH<sub>2</sub>CMe<sub>3</sub>]. Anal. Calcd for C<sub>21</sub>H<sub>29</sub>ClFNO: C 45.88, H 5.32, N 2.55. Found: C 46.04, H 5.11, N 2.29.

**12b**: <sup>1</sup>H NMR (400 MHz, C<sub>6</sub>D<sub>6</sub>): δ -2.61 (d, <sup>2</sup>J<sub>HH</sub> = 10.8 Hz, 1H, CH<sub>syn</sub>H), 1.26 (s, 15H, C<sub>5</sub>Me<sub>5</sub>), 1.55 (s, 15H, C<sub>5</sub>Me<sub>5</sub>), 5.54 (d, <sup>2</sup>J<sub>HH</sub> = 10.6 Hz, 1H, CH<sub>anti</sub>H), 6.51 (m, 1H, Ar H), 7.02 (m, 1H, Ar H), 8.05 (m, 1H, Ar H). <sup>19</sup>F{<sup>1</sup>H} NMR (282 MHz, C<sub>6</sub>D<sub>6</sub>): δ -41.5.

**Cp\*W(NO)(CH<sub>2</sub>CMe<sub>3</sub>)(C<sub>6</sub>H<sub>3</sub>FOMe) (13a,b)**. Complexes **13a** and **13b** resulted from the thermolysis of **1** (95.0 mg, 0.194 mmol) in *p*-fluoroanisole. The final dried product mixture was dissolved in a minimum of pentane, and the pentane solution was transferred to the top of a neutral activated alumina I column (2 × 7 cm) made up in pentane and supported on a medium-porosity frit. The column was eluted with 1:4 ether/pentane, whereupon **13b** (purple) eluted ahead of **13a** (red). Once the two bands had completely resolved, the eluant was changed to diethyl ether and the two bands were eluted and collected separately. Compounds **13a** and **13b** were recrystallized from 1:1 pentane/HMDS and 1:1 ether/HMDS, respectively, to obtain red irregularly shaped crystals (25 mg, 23%) of the former and purple diamond-shaped crystals (15 mg, 14%) of the latter.

**13a**: IR (cm<sup>-1</sup>): ν(NO) 1597 (s). <sup>1</sup>H NMR (400 MHz, C<sub>6</sub>D<sub>6</sub>): δ -2.93 (dd, <sup>2</sup>J<sub>HH</sub> = 11.9 Hz, <sup>5</sup>J<sub>HF</sub> = 6.1 Hz, 1H, CH<sub>syn</sub>H), 1.26 (s, 9H, CMe<sub>3</sub>), 1.63 (s, 15H, C<sub>5</sub>Me<sub>5</sub>), 3.44 (s, 3H, OMe), 5.48 (d, <sup>2</sup>J<sub>HH</sub> = 11.9 Hz, 1H, CH<sub>anti</sub>H), 6.63 (m, 1H, Ar H), 6.83 (m, 1H, Ar H), 7.91 (m, 1H, Ar H). <sup>19</sup>F{<sup>1</sup>H} NMR (282 MHz, C<sub>6</sub>D<sub>6</sub>): δ -17.0. MS (LREI, *m/z*, probe temperature 100 °C): 545 [M<sup>+</sup>], 488 [M<sup>+</sup> - CMe<sub>3</sub>]. Anal. Calcd for C<sub>22</sub>H<sub>32</sub>FNO<sub>2</sub>W: C 48.45, H 5.91, N 2.57. Found: C 48.70, H 6.22, N 2.81.

**13b**: IR (cm<sup>-1</sup>): ν(NO) 1561 (s). <sup>1</sup>H NMR (400 MHz, C<sub>6</sub>D<sub>6</sub>): δ -2.79 (d, <sup>2</sup>J<sub>HH</sub> = 11.6 Hz, 1H, CH<sub>syn</sub>H), 1.30 (s, 9H, CMe<sub>3</sub>), 1.62 (s, 15H, C<sub>5</sub>Me<sub>5</sub>), 3.05 (s, 3H, OMe), 5.04 (d, <sup>2</sup>J<sub>HH</sub> = 11.9 Hz,

1H,  $CH_{anti}H$ ), 6.30 (m, 1H, Ar H), 6.80 (m, 1H, Ar H), 8.25 (m, 1H, Ar H).  $^{19}F\{^1H\}$  NMR (282 MHz,  $C_6D_6$ ):  $\delta$  -48.0. MS (LREI,  $m/z$ , probe temperature 100 °C): 545 [ $M^+$ ], 488 [ $M^+ - CMe_3$ ]. Anal. Calcd for  $C_{22}H_{32}FNO_2W$ : C 48.45, H 5.91, N 2.57. Found: C 48.65, H 5.84, N 2.38.

**Cp\*W(NO)(CH<sub>2</sub>CMe<sub>3</sub>)(C<sub>6</sub>H<sub>3</sub>ClOMe) (14a,b).** Complexes **14a** and **14b** were formed by the thermolysis of **1** (87.0 mg, 0.177 mmol) in *p*-chloroanisole. At the end of the 40 h reaction period, the reaction vessel was wrapped in aluminum foil, and *p*-chloroanisole (bp 200 °C) was removed in vacuo at 70 °C. The dried product mixture was dissolved in a minimum of pentane, and the pentane solution was transferred to the top of a neutral activated alumina I column (2 × 7 cm) made up in pentane and supported on a medium-porosity frit. Elution of the column with 1:3 ether/pentane resulted in the development of two well-resolved bands as **14a** (purple) eluted ahead of **14b** (red). At this point, the eluant was changed to diethyl ether, and the two bands were eluted and collected separately. Compounds **14a** and **14b** were recrystallized from 1:1 ether/HMDS and HMDS to obtain purple plates (55 mg, 55%) and red plates (9 mg, 9%), respectively.

**14a:** IR (cm<sup>-1</sup>)  $\nu(NO)$  1584 (s).  $^1H$  NMR (400 MHz,  $C_6D_6$ ):  $\delta$  -2.86 (d,  $^2J_{HH} = 11.0$  Hz, 1H,  $CH_{syn}H$ ), 1.30 (s, 9H,  $CMe_3$ ), 1.54 (s, 15H,  $C_5Me_5$ ), 3.07 (s, 3H, OMe), 5.07 (d,  $^2J_{HH} = 11.0$  Hz, 1H,  $CH_{anti}H$ ), 6.28 (d,  $^3J_{HH} = 8.0$  Hz, 1H, Ar H), 7.12 (dd,  $^3J_{HH} = 8.0$  Hz,  $^4J_{HH} = 1.2$  Hz, 1H, Ar H), 8.45 (d,  $^4J_{HH} = 1.2$  Hz, 1H, Ar H).  $^{13}C\{^1H\}$  (100 MHz,  $C_6D_6$ ):  $\delta$  9.9 ( $C_5Me_5$ ), 33.8 ( $CH_2CMe_3$ ), 41.4 ( $CH_2CMe_3$ ), 54.5 (OMe), 110.4 (Ar C) 110.7 ( $C_5Me_5$ ), 127.2 (Ar C), 128.6 (Ar C), 131.2 ( $CH_2CMe_3$ ), 139.9 (Ar C), 158.5 (Ar C), 170.2 ( $WC_{ipso}$ ). MS (LREI,  $m/z$ , probe temperature 100 °C): 561 [ $M^+$ ], 504 [ $M^+ - CMe_3$ ]. Anal. Calcd for  $C_{22}H_{32}ClNO_2W$ : C 47.03, H 5.74, N 2.49. Found: C 46.85, H 6.08, N 2.88.

**14b:** IR (cm<sup>-1</sup>):  $\nu(NO)$  1567 (s).  $^1H$  NMR (400 MHz,  $C_6D_6$ ):  $\delta$  -2.42 (d,  $^2J_{HH} = 11.0$  Hz, 1H,  $CH_{syn}H$ ), 1.30 (s, 9H,  $CMe_3$ ), 1.63 (s, 15H,  $C_5Me_5$ ), 3.43 (s, 3H, OMe), 5.44 (d,  $^2J_{HH} = 11.0$  Hz, 1H,  $CH_{anti}H$ ), 6.57 (d,  $^3J_{HH} = 8.0$  Hz, 1H, Ar H), 7.21 (dd,  $^3J_{HH} = 8.0$  Hz,  $^4J_{HH} = 1.6$  Hz, 1H, Ar H), 7.93 (d,  $^4J_{HH} = 1.6$  Hz, 1H, Ar H). MS (LREI,  $m/z$ , probe temperature 100 °C): 561 [ $M^+$ ], 504 [ $M^+ - CMe_3$ ].

**[Et<sub>4</sub>N]<sup>+</sup>[Cp\*W(NO)(CH<sub>2</sub>CMe<sub>3</sub>)(CN)(*o*-C<sub>6</sub>H<sub>4</sub>F)]<sup>-</sup> ([Et<sub>4</sub>N]<sup>+</sup>[15]<sup>-</sup>).** A 4 dram vial was charged with **2a** (103 mg, 0.200 mmol), Et<sub>4</sub>NCN (31.1 mg, 0.199 mmol), MeNO<sub>2</sub> (5 mL), and a small magnetic stir bar. The mixture was stirred for 5 min at room temperature, whereupon it rapidly turned yellow. The solvent was then removed in vacuo, and the yellow waxy residue was washed with pentane (2 × 5 mL). The remaining solid was redissolved in a minimum amount of THF, and diethyl ether was carefully layered on top of the solution. Storage of this mixture at -30 °C overnight resulted in the deposition of yellow irregularly shaped crystals of **[Et<sub>4</sub>N]<sup>+</sup>[15]<sup>-</sup>** (90 mg, 67%).

**[Et<sub>4</sub>N]<sup>+</sup>[15]<sup>-</sup>:** IR (cm<sup>-1</sup>):  $\nu(CN)$  2103 (s),  $\nu(NO)$  1530 (s).  $^1H$  NMR (400 MHz, acetone-*d*<sub>6</sub>):  $\delta$  0.69, 1.42 (d,  $^2J_{HH} = 11.1$  Hz, 2H,  $CH_2CMe_3$ ), 1.15 (s, 9H,  $CMe_3$ ), 1.34, (tt, 12H,  $CH_3CH_2$ ), 1.63 (s, 15H,  $C_5Me_5$ ), 3.29 (q, 8H,  $CH_3CH_2$ ), 6.66 (m, 1H, Ar H), 6.73 (m, 1H, Ar H), 6.86 (m, 1H, Ar H), 8.04 (m, 1H, Ar H).  $^{19}F\{^1H\}$  NMR (282 MHz,  $C_6D_6$ ):  $\delta$  -1.2. MS (LSIM):  $m/z$  541 [ $M^-$ ]. Anal. Calcd for  $C_{30}H_{50}FN_3OW$ : C 53.65, H 7.50, N 6.26. Found: C 53.61, H 7.37, N 6.39.

**Cp\*W(NO)( $\eta^2-C(=O)CH_2CMe_3$ )(*o*-C<sub>6</sub>H<sub>4</sub>F) (16).** A Schlenk tube was charged with **2a** (50.0 mg, 0.101 mmol), and hexanes (10 mL) were added via syringe to obtain a red solution. CO (1 atm) was bubbled through this solution for 5 min, whereupon it turned yellow and a yellow precipitate deposited. The solvent was removed in vacuo, and the residue was washed with cold pentane (2 × 3 mL). The solid was then redissolved in a minimum of diethyl ether, and pentane was carefully layered on top. The mixture was stored at -30 °C overnight to induce the deposition of yellow feathery crystals of **16** (40 mg, 76%).

**16:** IR (cm<sup>-1</sup>): 1584 (s), 1566 (s).  $^1H$  NMR (400 MHz,  $C_6D_6$ ):  $\delta$  0.92 (s, 9H,  $CMe_3$ ), 1.66 (s, 15H,  $C_5Me_5$ ), 2.67 (d,  $^2J_{HH} = 13.2$  Hz, 1H,  $CH_2CMe_3$ ), 2.98 (d,  $^2J_{HH} = 13.2$  Hz, 1H,  $CH_2CMe_3$ ), 7.07–7.14 (m, 3H, Ar H), 8.20 (m, 1H, Ar H).  $^{19}F\{^1H\}$  NMR (282 MHz,  $C_6D_6$ ):  $\delta$  -12.0. MS (LREI,  $m/z$ , probe temperature 100 °C): 543 [ $M^+$ ], 486 [ $M^+ - CMe_3$ ]. Anal. Calcd for  $C_{22}H_{30}FNO_2W$ : C 48.63, H 5.57, N 2.58. Found: C 48.99, H 5.77, N 2.60.

**X-ray Crystallography.** Data collection for each compound was carried out at -100 ± 1 °C on either a Rigaku AFC7/ADSC CCD diffractometer or a Bruker X8 APEX diffractometer, using graphite-monochromated Mo K $\alpha$  radiation.

Data for **2a** were collected to a maximum  $2\theta$  value of 55.8° in 0.5° oscillations with 8.0 s exposures. The structure was solved by direct methods<sup>23</sup> and expanded using Fourier techniques. All non-hydrogen atoms were refined anisotropically; hydrogen atoms H07A and H07B were refined isotropically, and all other hydrogen atoms were included in fixed positions. The final cycle of full-matrix least-squares analysis was based on 4883 observed reflections and 243 variable parameters.

Data for **5a** were collected to a maximum  $2\theta$  value of 55.8° in 0.5° oscillations with 35.0 s exposures. The structure was solved by direct methods<sup>23</sup> and expanded using Fourier techniques. All non-hydrogen atoms were refined anisotropically; hydrogen atoms H08A and H08B were refined isotropically, and all other hydrogen atoms were included in fixed positions. The final cycle of full-matrix least-squares analysis was based on 4666 observed reflections and 252 variable parameters.

Data for **6a** were collected to a maximum  $2\theta$  value of 55.6° in 0.5° oscillations with 10.0 s exposures. The structure was solved by direct methods<sup>23</sup> and expanded using Fourier techniques. All non-hydrogen atoms were refined anisotropically; hydrogen atoms H15A and H15B were refined isotropically with fixed bond distances, and all other hydrogen atoms were included in fixed positions. The final cycle of full-matrix least-squares analysis was based on 5848 observed reflections and 305 variable parameters.

Data for **7** were collected to a maximum  $2\theta$  value of 55.7° in 0.5° oscillations with 20.0 s exposures. The structure was solved by direct methods.<sup>24</sup> All hydrogen atoms were included in calculated positions but not refined, except H11, which was found in a difference map and refined isotropically. The final cycle of full-matrix least-squares analysis was based on 5404 reflections and 287 variable parameters.

Data for **10c** were collected to a maximum  $2\theta$  value of 56.0° in 0.5° oscillations with 6.0 s exposures. The structure was solved by direct methods<sup>23</sup> and expanded using Fourier techniques. All non-hydrogen atoms were refined anisotropically; hydrogen atoms H7A and H7B were refined isotropically, and all other hydrogen atoms were included in fixed positions. The final cycle of full-matrix least-squares analysis was based on 4972 observed reflections and 251 variable parameters.

Data for **16** were collected to a maximum  $2\theta$  value of 55.5° in 0.5° oscillations with 10.0 s exposures. The structure was solved by direct methods.<sup>24</sup> The fluorobenzyl ligand was disordered in two orientations. Restraints were used to maintain both reasonable geometries for both benzyl fragments and both C–F distances. The carbon atoms of the minor disordered fragment were refined with isotropic thermal parameters; all other non-hydrogen atoms were refined anisotropically. All hydrogen atoms were included in calculated positions but not refined. The final cycle of full-matrix least-squares refinement on  $F^2$  was based on 5031 reflections and 262 variable parameters.

(23) SIR92: Altomare, A.; Cascarano, M.; Giacovazzo, C.; Guagliardi, A. *J. Appl. Crystallogr.* **1993**, *26*, 343.

(24) SIR97: Altomare, A.; Burla, M. C.; Cammali, G.; Cascarano, M.; Giacovazzo, C.; Guagliardi, A.; Moliterni, A. G. G.; Polidori, G.; Spagna, A. *J. Appl. Crystallogr.* **1999**, *32*, 115.

Table 1. X-ray Crystallographic Data for Complexes 2a, 5a, 6a, 7, 10c, and 16

	2a	5a	6a
Crystal Data			
empirical formula	C <sub>21</sub> H <sub>30</sub> FNO <sub>2</sub> W	C <sub>22</sub> H <sub>33</sub> NO <sub>2</sub> W	C <sub>29</sub> H <sub>35</sub> NOW
cryst habit, color	irregular, red	prism, dark red	plate, purple
cryst size (mm)	0.30 × 0.15 × 0.09	0.50 × 0.50 × 0.10	0.20 × 0.15 × 0.05
cryst syst	triclinic	monoclinic	triclinic
space group	P $\bar{1}$	P2 <sub>1</sub> /n	P $\bar{1}$
volume (Å <sup>3</sup> )	1041.71(19)	2143.2(3)	1284.4(2)
a (Å)	8.2185(9)	10.6196(11)	8.8372(8)
b (Å)	9.2843(9)	18.1403(13)	9.1967(8)
c (Å)	14.5576(15)	11.2112(10)	16.620(2)
α (deg)	74.260(4)	90	75.253(4)
β (deg)	89.287(4)	97.101(3)	79.602(4)
γ (deg)	77.311(4)	90	88.771(4)
Z	2	4	2
density (calcd) (Mg/m <sup>3</sup> )	1.643	1.634	1.545
absorp coeff (cm <sup>-1</sup> )	55.61	54.05	45.17
F <sub>000</sub>	508	1048	596
Data Collection and Refinement			
measd reflns: total	34 992	18 559	56 192
measd reflns: unique	4883	4666	5848
final R indices <sup>a</sup>	R1 = 0.0221, wR2 = 0.0586	R1 = 0.0356, wR2 = 0.0925	R1 = 0.0245, wR2 = 0.0686
GOF on F <sup>2b</sup>	1.092	1.096	1.212
largest diff peak and hole (e <sup>-</sup> Å <sup>-3</sup> )	1.963 and -1.918	4.605 and -3.493	1.282 and -1.263
Crystal Data			
empirical formula	C <sub>27</sub> H <sub>45</sub> NOW	C <sub>21</sub> H <sub>29</sub> F <sub>2</sub> NOW	C <sub>22</sub> H <sub>30</sub> FNO <sub>2</sub> W
cryst habit, color	platelet, orange-red	rod, red	needle, yellow
cryst size (mm)	0.20 × 0.20 × 0.05	0.50 × 0.20 × 0.20	0.40 × 0.12 × 0.03
cryst syst	monoclinic	triclinic	monoclinic
space group	P2 <sub>1</sub> /n	P $\bar{1}$	P2 <sub>1</sub> /n
volume (Å <sup>3</sup> )	2565.9(3)	1047.99(15)	2159.2(4)
a (Å)	10.792(1)	8.0777(6)	11.8892(15)
b (Å)	16.440(1)	9.4908(8)	15.8619(18)
c (Å)	14.468(1)	14.7275(13)	12.0429(14)
α (deg)	90	72.039(3)	90
β (deg)	91.629(3)	89.092(2)	108.061(5)
γ (deg)	90	77.726(2)	90
Z	4	2	4
γ (deg)	90	77.726(2)	90
density (calcd) (Mg/m <sup>3</sup> )	1.510	1.690	1.671
absorp coeff (cm <sup>-1</sup> )	45.19	55.37	53.74
F <sub>000</sub>	1184	524	1072
Data Collection and Refinement			
measd reflns: total	22 737	20 467	28 754
measd reflns: unique	5404	4972	5031
final R indices <sup>a</sup>	R1 = 0.037, wR2 = 0.081	R1 = 0.0126, wR2 = 0.0310	R1 = 0.055, wR2 = 0.067
GOF on F <sup>2b</sup>	1.12	1.052	1.031
largest diff peak and hole (e <sup>-</sup> Å <sup>-3</sup> )	2.42 and -1.74	0.691 and -0.496	2.29 and -0.98

<sup>a</sup> R1 on F =  $\sum(|F_o| - |F_c|)/\sum|F_o|$  ( $I_o > 2\sigma I_o$ ); wR2 =  $[\sum(F_o^2 - F_c^2)^2/\sum w(F_o^2)^2]^{1/2}$  (all data); w =  $[\sigma^2 F_o^2]^{-1}$ . <sup>b</sup> GOF =  $[\sum w(|F_o| - |F_c|)^2/\text{degrees of freedom}]^{1/2}$ .

For each structure neutral-atom scattering factors were taken from Cromer and Waber.<sup>25</sup> Anomalous dispersion effects were included in  $F_{\text{calc}}$ ;<sup>26</sup> the values for  $\Delta f'$  and  $\Delta f''$  were those of Creagh and McAuley.<sup>27</sup> The values for mass attenuation coefficients are those of Creagh and Hubbell.<sup>28</sup> All calculations were performed using the CrystalClear software package of Rigaku/MSU,<sup>29</sup> or SHELXL-

97.<sup>30</sup> X-ray crystallographic data for all six structures are presented in Table 1, and full details of all crystallographic analyses are provided in the Supporting Information.

**Acknowledgment.** We are grateful to the Natural Sciences and Engineering Research Council of Canada and the Killam Program for the Canada Council for the Arts for financial support of this work. We also acknowledge E. Tran for conducting some preliminary studies, and we thank C. J. Semiao for technical assistance.

**Supporting Information Available:** CIF files providing full details of crystallographic analyses of complexes **2a**, **5a**, **6a**, **7**, **10c**, and **16**. This material is available free of charge via the Internet at <http://pubs.acs.org>.

OM060390J

(25) Cromer, D. T.; Waber, J. T. *International Tables for X-ray Crystallography*; Kynoch Press: Birmingham, 1974; Vol. IV.

(26) Ibers, J. A.; Hamilton, W. C. *Acta Crystallogr.* **1964**, *17*, 781.

(27) Creagh, D. C.; McAuley, W. J. *International Tables for X-ray Crystallography*; Kluwer Academic Publishers: Boston, 1992; Vol. C.

(28) Creagh, D. C.; Hubbell, J. H. *International Tables for X-ray Crystallography*; Kluwer Academic Publishers: Boston, 1992; Vol. C.

(29) *CrystalClear*, Version 1.3.5b20; Molecular Structure Corp.: The Woodlands, TX, 2002.

(30) Sheldrick, G. M. *SHELXL97*; University of Göttingen: Germany, 1997.